REPORT DOCUMENTATION PAGE

Form Approved
OMB No. 0704-0188

1. AGENCY USE ONLY (Leave blank)	2. REPORT DATE	3. REPORT TYPE AND DATES COVERED
		Technical Report

4. TITLE AND SUBTITLE

Poly (p-phenylene vinylene) as Alignment Layers in Liquid Crystal Displays (LCD's) via the Langmuir-Blodgett Technique

5. FUNDING NUMBERS

Grant N0014-94-1-0270
R&T Code 31321 01
Kenneth Wynne

6. AUTHOR(S)

Andy C. Chang[1], Matthew J. Ebersbach[1], Masa-Aki Kakimoto[3], D. Johnson[4], J. A. Mann, jr.[2], Jerome B. Lando[1]*

7. PERFORMING ORGANIZATION NAME(S) AND ADDRESS(ES)

[1]Case Western Reserve University, Dept. of Macromolecular Sci. & Engr. Cleveland, OH 44106; [2]Case Western Reserve University, Dept. of Chemical Engineering, Cleveland OH 44106; [3]Tokyo Institute of Technology, Meguro-ku, Tokyo 152 (Japan) Dept. of Organic and Polymeric Materials; [4]Kent State, Center for Liquid Crystals and Physics, Kent OH 44242

8. PERFORMING ORGANIZATION REPORT NUMBER

13

9. SPONSORING / MONITORING AGENCY NAME(S) AND ADDRESS(ES)

Department of the Navy
Office of Naval Research
800North Quincy Street
Arlington, VA 22217-5000

10. SPONSORING / MONITORING AGENCY REPORT NUMBER

11. SUPPLEMENTARY NOTES

12a. DISTRIBUTION / AVAILABILITY STATEMENT

Reproduction in whole or in part is permitted for any purpose of the United States Government. This document has been approved for public release and sale; its distribution is unlimited.

12b. DISTRIBUTION CODE

13. ABSTRACT *(Maximum 200 words)*

Preparation of alignment layers of PPV via the poly (p-xylene-α-diethyl sulphonium perfluorononanoate) precursor has demonstrated initial success. However, UV-vis and grazing angle X-ray techniques have shown that the precursor collapses by centrosymmetric multilayer formation at 25 mN / m and 13°C. At these conditions, Z-type deposition on hydrophilic glass results in an irregular lamination / delamination process after 3 iterations. IR measurements have shown nearly complete conversion to PPV by thermal elimination. UV measurements, however, were not found to be representative of the proportion of converted to unconverted units.

14. SUBJECT TERMS

15. NUMBER OF PAGES

16. PRICE CODE

17. SECURITY CLASSIFICATION OF REPORT	18. SECURITY CLASSIFICATION OF THIS PAGE	19. SECURITY CLASSIFICATION OF ABSTRACT	20. LIMITATION OF ABSTRA
Unclassified	Unclassified	Unclassified	UL

Poly (p-phenylene vinylene) as Alignment Layers in Liquid Crystal Displays (LCD's) via the Langmuir-Blodgett Technique

Andy C. Chang, Matthew J. Ebersbach, Masa-Aki Kakimoto[a], D. Johnson[b]
J. A. Mann, Jr.[c] and Jerome B. Lando*
Department of Macromolecular Science, [c]Department of Chemical Engineering
Case Western Reserve University, Cleveland OH 44106
[b]Department of Physics, Kent State University, Kent OH and
[a]Department of Textile and Polymeric Materials, Tokyo Institute of Technology,
Ookayana, Meguro-ku, Tokyo 152 Japan

Abstract

Preparation of alignment layers of PPV via the poly (p-xylene-α-diethyl sulphonium perfluorononanoate) precursor has demonstrated initial success. However, UV-vis and grazing angle X-ray techniques have shown that the precursor collapses by centrosymmetric multilayer formation at 25 mN / m and 13°C. At these conditions, Z-type deposition on hydrophilic glass results in an irregular lamination / delamination process after 3 iterations. IR measurements have shown nearly complete conversion to PPV by thermal elimination. UV measurements, however, were not found to be representative of the proportion of converted to unconverted units.

[b]Deceased

Introduction

Conjugated polymers such as poly (p-phenylene vinylene) (PPV) differ most prominently from other organic compounds in the property of electrical conductivity. Most organic compounds have conductivies on the scale of $10^{-9}(\Omega \cdot m)^{-1}$ or lower while values approaching $2000(\Omega \cdot m)^{-1}$ have been reported for Na doped PPV.[1] There has been speculation on applications which would benefit from a lightweight, low-cost, plastic conductor. As a result, there has been much work in recent years to elucidate the mechanisms by which conduction occurs in polymers and to design materials which exhibit high conductivities while retaining the mechanical properties associated with polymers.

Highly conjugated organic systems owe their high conductivity to the low energy required to excite their delocalized π-electron to antibonding orbitals. To maintain p_z-orbital overlap, the molecules need to assume near planar conformations. This restriction in most systems reduces the mechanical properties typically identified with polymers.

Electronic and optical devices, however, do not require the strength and toughness associated with other applications. One aspect of such devices, liquid crystal alignment, is one of the first successes in the incorporation of organic materials in information systems. Hiltrop and Stegemyer were the first to successfully use lecithin films to align liquid crystals.[2]

The alignment layer is what is used to control liquid crystal orientation in the unswitched state. An organic layer with surface orientation is normally used. In industry, thin layers of polyimide are rubbed with a cloth coated rotor.[3] This process produces microtrenches in the surface and unbalanced charges in the direction of rubbing which interact to orient the dipole of the liquid crystal.[4] Rubbing is a violent process which tends to introduce foreign particles and damage fine electrodes.[5] As display needs become more sophisticated, this technique becomes less adequate and necessitates investigation into other means of liquid crystal alignment.

Much recent work has been done in characterization of PPV precursors, PPV, and doped PPV. To probe the electronic structure of doped and undoped PPV, several research groups have conducted electroluminescence and photoluminescence studies.[6,7,8,9,10] Knowledge of the electronic structure, photoexcitation, the behavior of injected carriers, and the mechanism of conduction is important in LED's and other electronic devices. Infrared and Raman spectroscopy in conjunction with dynamic modeling has been used by Buisson and co-workers to assign Raman and IR modes and to calculate force constants for undoped and $FeCl_3$ doped polymer.[11] Bradley and co-workers have used IR on bulk stretched films to monitor crystallinity and orientation during the conversion process of poly (p-xylene-α-dimethyl sulphonium chloride).[12] Effective conjugation coordinate theory (ECC) has been applied by Tian, Zerbi, and Müllen to explain the observed intensities and frequencies of the modes and transitions observed in IR and Raman spectroscopy for the doped and undoped samples in relation to the delocalization of the $\Pi-$electrons.[13] They have also used UV, visible, and vibrational data in conjunction with modified neglect or differential overlap (MNDO) modeling to suggest that short PPV oligomers are twisted in noncrystalline phases but almost coplanar in the crystalline phase of their stretched films.[14]

Since PPV has a conjugated backbone, UV - visible spectroscopy has proven to be quite useful though the results have not been completely explained. Woo has compared the absorption spectra of short model oligomers of PPV with those of higher molecular

weights to conclude that delocalization is on the order of 10 to 17 repeat units.[15] However, Karasz's data from semi-empirical models suggest that the lowest energy transition ($\lambda = 402$ nm) in the UV - visible spectrum does not correspond to the $\Pi - \Pi^*$ transition of the conjugated backbone.[16] Instead, he suspects this absorption to result from overlapping transitions of localized energy levels. In short, his point is that UV data are not representative of extensive delocalization along the backbone. Other researchers have also observed the convergence of absorbances, emission, and photoconductivity maxima after four repeat units.[17,18,19,20,21]

The morphology of bulk PPV films has been studied by Bradley and Capistran.[22,23,24] The surface and morphology of LB films of PPV have been studied by Kakimoto.[25] SEM studies by his group found both the poly (p-xylene-α-diethyl sulphonium perfluorononanoate) precursor and converted polymer to be flat, smooth, and free of defects.

Introduction of *p* and *n* type dopants to PPV and other conjugated polymers is known to increase conductivity. Researchers have investigated the effects of doping PPV with Na, I, H_2SO_4, SO_3, AsF_5, $FeCl_3$, and sodium napthalide.[26,27,28,29,30,31,32]

This paper reports the initial work in a project to make use of the orientation inherently produced by the LB technique in polymeric systems and the high conductivity associated with doped conjugated systems such as PPV. The intent is to combine the functions of the alignment layer and electrode into a single film of PPV. Not only will this eliminate the need for two films but it should also allow for LCD patterning by selective area conversion of the precursor to PPV.

Experimental

The device in which we carry out our experiments is the Lauda Film Balance ($70 \times 15 \times 0.7$ cm). The trough is teflon coated and the barriers are made from machined teflon. Barrier position is measurable to within ± 0.3 cm. Uncertainty in pressure measurements is ± 0.2 mN / m.

The spreading solution was prepared in the following manner. Aqueous solutions of poly(p-xylene-α-diethylsulfonium chloride) were diluted to 2 mM with ethanol . This solution was subsequently diluted to 1 mM with 1,1,1-trichloroethane. The side chain was attached in an ion exchange reaction when the solution was mixed with an equal

volume of 1 mM $NaC_8F_{17}COO$ solvated in a 1:1 solution of ethanol : 1,1,1-trichloroethane. This mixed solvent system has been used in order to solvate the main and side chain while keeping the overall solution insoluble enough to spread onto the water surface. The subphase used in these experiments was water purified by a Milli-Q water system.

After spreading 100μL onto 322.5 cm^2 of water surface (approximately 200% of the estimated co-area) using a Drummond Micropipette, 15 minutes was allowed to elapse in order for the solvents to evaporate. While monitoring pressure, the moving barrier was compressed at 2 cm / min until it was within 6 cm of the floating barrier (90 cm^2 remaining area). This is the lower limit of the system.

Compressive creep measurements were done by compressing the films and stopping the barrier when the target pressure was reached. Constant pressure was maintained using the pressure controller. An IBM PC was used to measure molecular area versus time. Temperature was set at 13°C.

For deposition, the pressure was increased to 25 mN/m using the same compression speed and maintained by pressure controller circuitry in the film balance control. Deposition was done using a dipping apparatus consisting of a stepper motor geared to an arm to which substrates were attached.

Holding pressure at 25 mN/m, the film was allowed to stabilize for 20 minutes. The computer was programmed to move the substrate in and out of the subphase at 5 mm / min. The type of substrate used varied with the type of characterization experiment that was being done. These include glass, fused quartz, ZnSe, and copper electron diffraction grids. A 20 minute interval was allowed to pass between interations in order for the film to dry.

UV-vis absorbance spectroscopy is a useful tool for studying electronic transitions in conjugated compounds. Both the precursor and PPV absorb in the UV-vis range making such spectra a natural tool for characterizing this polymer system. Fused quartz was used for its low absorbance in the 190 to 650 nanometer range. Measurements were made with a Varian Cary UV-Visible Spectrophotometer.

In this system, we have used IR to confirm the identity and configuration of the compounds and to subsequently determine the extent of reaction. For these measurements, the precursor was deposited onto ZnSe slides and analyzed with a Bio-Rad FT-60 in transmission mode with background subtraction. To get adequate

absorbances, a thick sample of 100 depositions was used for these experiments. 1024 scans were used to get acceptable signal to noise ratios.

A Philips x-ray diffractometer (CuKα, 1.5418 Å) in the reflection mode was used to determine layer spacing. Samples were deposited onto glass for x-ray characterization. Other experimental parameters include a 0.05° step, a 38 second integration time, and the use of the $\frac{1}{12}^{\circ}$ slit.

The technique established by Wessling and Zimmerman consists of synthesis of a polysulfonium salt followed by thermal elimination to yield high molecular weight PPV.[33,34] It has been proposed that this conversion reaction occurs by an E1 mechanism.[35] For our precursor, a carbocation intermediate forms which subsequently decomposes to PPV by elimination of the dialkyl sulfide moiety and $C_8F_{17}COOH$.

The main advantage of using this precursor is increased processibility. Bulk processing of this precursor has been investigated by Karasz in conductivity experiments.[37] Application of the LB method was first investigated by Kakimoto.[37] It is his system of attaching the perfluoronated side chain which we have used in this study.

The conversion reaction was done in a vacuum oven (1 kPa) at various temperatures ranging from 200 to 400°C. Before placing the samples into the vacuum oven , the chamber was flushed three times with nitrogen gas to remove the maximum amount of oxygen. Oxygen is known to oxidize the vinylene carbons producing carbonyl moieties.[38] The lowest energy UV-vis absorbance peak was found not to change after 7 hours for temperatures from 230 to 250°C.

Doping with $FeCl_3$ solvated in dichloromethane was done according to the procedure outlined by Piaggio for poly (p-phenylene sulfide).[39] After conversion to PPV, the films were doped by placing the samples in dry dichloromethane. $FeCl_3$ was added in small amounts until the solution was saturated (approximately 0.1 M). The solution was green in color. A stirring rod was placed in the container with the sample solution which in turn was placed in a dessicator placed on top of a magnetic stirrer. Dry nitrogen was continually passed over the solution to prevent solvation of water. The film was allowed to be doped for 1 hour. Afterwards, excess $FeCl_3$ was rinsed off with a little more dry dichloromethane. The sample was then allowed to dry in open air.

A Brewster angle microscope was used to obtain images on the order of 1 μm. This instrument consists of a 10 milliwatt HeNe laser (500:1 polarization, 632.8 nm) which passes through a quarter - wave plate, strikes the film at the Brewster angle (53°), and is reflected by a mirror to a CCD camera. The image is digitized and stored on a Macintosh personal computer.

Conductivity measurements were done using the standard 4 probe method. The instrumentation consists of a Hewlett-Packard 3478A multimeter, a Keithley 2220 Programmable Current Source, a Keithley 182 Sensitive Digital Voltmeter, and a Signatone 4 Contact probe. Samples used in these measurements were also deposited onto glass slides. Gold electrodes of 500Å were sputtered onto the films.

Alignment cells were made using film samples on glass slides. These slides were epoxied together with dipping directions antiparallel and 20 μm polyethylene spacers at the edges. 5CB liquid crystal was allowed to flow into the gap. The remaining edges were sealed using more epoxy. Twisted nematic cells were made in the same manner except with the dipping directions oriented at 90°.

Results and Discussion

I. Isotherms and compressive creep properties

Figure 1 is the $\pi - area$ isotherm of the PPV precursor at 13.5°C. This plot of pressure versus molecular area shows a gradually rising curve and a fairly low modulus. Collapse is at 46 mN/m. Further compression does not cause an increase in pressure after this point. Extrapolation of this curve yields a co-area of 0.59 nm^2 / repeat unit.

Collection of isotherms at temperatures from 8 to 25°C gives approximately the same curve with small differences that are within experimental uncertainty of position, pressure, and solution concentration. The low Gibb's elastic modulus of the gradually rising curve and the high co-area are indicative of open packing. A plateau-like shape without further increase in pressure indicates ductile collapse. Formation of multilayers in some materials is often accompanied by rising pressure after initial collapse. This was not observed for the PPV-precursor.

The compressive creep behavior of the PPV-precursor was found to be highly dependent upon temperature. At temperatures above 15.5°C, the film quickly creeps to 0 nm^2 / repeat unit at rates typically higher than -100% per hour. Below 15°C, the film shows a dramatic improvement in stability. The temperature used for all creep and

deposition experiments was 13°C. Compressive creep versus time plots are shown in figure 2. Initially, the film shows a slightly faster creep but quickly reaches a steady state creep rate averaging -5% / hour. It is suspected that solvation of the film into the subphase and multilayer formation are the mechanisms by which molecular area is lost. Solvation is evidenced by the irregular dewetting of the trough surface during cleaning after each experiment. Evidence of multilayer formation is discussed in section VII.

Further attempts at increasing film stability by varying the pH, ionic content, and temperature of the subphase were not successful. These include acidifying the subphase up to 5 M HNO_3, use of 0.1 M $NaCl_{(aq)}$, and decreasing the temperature down to 8°C (the practical lower limit of the temperature controller). Decreasing the temperature below 15 °C and down to 8°C gave no improvement in the -5% / hour creep rate.

The PPV - precursor film was found to be very sensitive to disturbances. The -5% / hour creep rate was achieved only after careful adjustment of the pressure controller damping factor and fine tuning of the vibration isolation devices.

II. Transfer Ratio Measurements

Since the PPV precursor film creeps, it had been difficult to gauge exactly when film deposition occurred, how much of the film was being deposited onto the substrate, and what quantity was lost to the mechanisms responsible for creep. As a result, measurements of transfer ratio for a creeping film posed quite a challenge. However, since it appears that the rates of the creep mechanisms are unaffected by the dipping process, we can subtract the creep from the barrier displacement to calculate how much of the film would be deposited if no creep were present. Figure 3 is a dual plot of dipper position and moving barrier position as the deposition process occurs. The line with filled points shows dipper position. The program moves the dipper through a repeating series of positions: down to the water surface, below the water surface (negative positions), out of the water subphase (positive positions), and out of the trough to dry (the highest positive position). A record of the barrier position as the dipping process occurs shows that the dipper moves the quickest as the substrate is being removed from the subphase. At other stages of dipping, the barrier moves at approximately the same rate. This result implies Z-type deposition. Removal of the effect of creep is done by subtracting the barrier displacement on the downward cycle from the upward cycle while the substrate is within the water surface. The effect of the initial quicker creep is avoided by waiting 20 minutes before beginning deposition. The fluctuations in creep rate are long in comparison to the time required for the downward and upward stroke of the

deposition process. In substracting the film creep of the corresponding downward movement, we attempt to make the best guess as to how much creep occurs on the upward trip. Figure 4 shows the result of this calculation. Calculated transfer ratios using this method are centered around a value of 0.95 for the first 4 iterations.

For the temperature ranges at which deposition is done (between 8 and 15°C), the transfer ratio adjusted for creep does not measurably differ once proper set-up is achieved.

For iterations 6, 10, and 20, the moving barrier was observed to move away from the floating barrier during the downward trip of the substrate. This observation is indicative of material being introduced to the water surface since pressure is maintained constant by the pressure controller at all times. However, material was redeposited during the upward trip. When delamination/deposition occurs, the creep compensated calculation gives a transfer ratio greater than 1. Delamination and deposition of the precursor were observed for multilayers thicker than 5 depositions. Each experimental run results in 5 depositions. Longer drying times were not found to affect this process. The overall delamination / deposition process appears to be irregular.

III. Ultraviolet-Visible Absorbance Spectroscopy

UV-visible spectroscopy shows an absorbance at 196 nm corresponding to a $\Pi - \Pi^*$ transition of the phenyl ring in the precursor with poorly resolved absorbances centered at approximately 235 and 245 nm (see figure 5).[40] Plotting absorbance at 196 nm versus number of depositions shows a fairly linear relationship further supporting the result of the transfer ratio calculations (see figure 6). In short, deposition is repeatable and regular for the first 3 interations. The sharp break in slope after 3 depositions corresponds to the irregular deposition/delamination process discussed earlier in section II. However, a positive net deposition is evidenced by a positive _(absorbance) / _(deposition) value after 3 depositions. This result is confirmed visually by slides which are visually more yellow-orange after heating than samples which have undergone fewer deposition cycles.

Taking the spectra again for the films after the heat treatment reveals peaks at 200 nm, 245 nm and a peak centered around 392 nm (see figure 7). The peak absorbances at 200 nm corresponds to previously mentioned $\Pi - \Pi^*$ transition. The broad absorbance centered about 392 nm corresponds to the absorbance of a system with increased conjugation.[41] Plotting this peak height against the number of depositions again shows a near linear correlation (see figure 8). This result demonstrates that conversion is fairly uniform from sample to sample. The relationship between (1 / conjugation length) and

the $\Pi - \Pi^*$ transition wavelength has been studied by Lhost for oligomers of PPV.[42] Plotting our peak absorbance of 392 nm on their data set corresponds to an average conjugation length of 5.2 repeat units for the thickest sample (see figure 9).

Seven hour heat treatments at temperatures higher than 285°C resulted in loss of conjugation (see figure 10). This degradation is suspected to be caused by reaction with residual oxygen gas present in the vacuum oven. In processing bulk samples, Murase and co-workers have reported that full conversion of the PPV precursor is only achieved at 300°C and above.[43]

IV. X-Ray Diffraction

X-ray diffraction at grazing angles gives out-of-plane spacings (see figure 11). Measurements of the precursor shows a single peak at $2\theta = 2.44°$. Calculation using Bragg's law indicates a layer repeat of 36.2 Å. This spacing is approximately twice the side chain length which shows that the chains are oriented centrosymmetrically about the chain axis to yield Y-type structure. A broad intensity centered about 25° (not pictured) corresponds to the amorphous peak of glass, the substrate used in these X-ray studies. It has been suggested that the co-area of $0.59\ nm^2$ / repeat unit corresponds to the side chains lying flat on the air-water interface.[44] Our X-ray diffraction measurements do not support this hypothesis.

Seven hours of heat treatment results in the peak at 2.44° diminishing and migrating toward smaller spacing. This indicates that significant conversion is taking place. After a total of 15 hours, the peak appears to completely vanish. This sample has a much fainter yellow appearance in contrast to the intense yellow of the PPV samples prepared for UV-vis and X-ray which were only treated for 7 hours. This is probably due to PPV degradation. The 7 hour treatment was arrived at using successive 1 hour treatments while monitoring the absorbance of the longest wavelength. Progressively higher temperatures were then tried. Migration to lower energies stopped after 7 hours at 235°C. Future plans include careful tracking of the elimination reaction versus times greater than 7 hours with both X-ray and UV-vis measurements.

V. Fourier Transform Infrared Absorbance Spectroscopy

FTIR spectra in the transmission mode show a rich assortment of peaks (see figure 12). Table 1 shows the peaks observed in this measurement and the assignments. Since this precursor in one form or another has been studied by other workers, their assignments are

referenced when appropriate. The other peak assignments were made by relating the observed absorbances to those in the standard reference by Bellamy that correspond in shape and intensity.[6]

The absorbance spectra of the side chain alone ($NaC_8F_{17}COO$) confirms most of these assignments (see figure 13).

Measurements taken after the heating process show relatively fewer peaks (see figure 14). Table 2 lists their locations, intensities, assignments, and references. Notably absent are the C-F modes centered at approximately 1100 cm^{-1}. Now present are well defined ring modes centered about 1500 cm^{-1}.

Dichroic ratio measurements for the observed peaks are 1. This result in conjunction with grazing angle X-ray diffraction suggest that the side chains are perpendicular to the substrate with no preferential orientation of the C-F bonds about the axis of the side chains.

VI. Conversion to PPV and Conjugation as Related by UV - Vis and FTIR

As mentioned earlier, the average conjugation of the films should be approximately 5.2 repeat units.[45] However, the IR spectrum of films which underwent the same 7 hour heat treatment show almost 100% elimination. There are several possible explanations for these results.

The first possibility is that both data sets are representative of the structure. 100% conversion is attained but residual oxygen present in the vacuum oven degrades the vinylene carbon of PPV as discussed earlier in the introduction. This possibility is supported by the presence of the peak at 1685 cm^{-1} in the precursor and the peak at 1695 cm^{-1} in the converted sample. We know that 1685 cm^{-1} corresponds to the carbonyl mode of the perfluoronated side chain. The 1695 cm^{-1} peak may be due to carbonyl products of the oxidized vinylene carbons. Verification of this would require using a side chain that does not have a carbonyl group. If the 1695 cm^{-1} peak is still present in the converted polymer, then degradation of the polymer by oxygen would be a possible explanation for high conversion with short conjugation length.

The second hypothesis is that degradation does not occur to a significant extent for a heat treatment of 7 hours at 250°C. As reported earlier, degradation is observed in our samples at approximately 285°C and in the samples of other workers above 400°C. What

could reconcile UV - vis and IR spectra is the explanation that the longest wavelength absorption at 392 nm does not correspond to a $\Pi - \Pi^*$ transition along the conjugation length of the entire backbone but to the overlap of localized energy levels. This was hypothesized by Karasz for the PPV system.[46] He suggests that this may be due the coupling of intramolecular vibrational and electronic transitions. In his semi-empiracle study, he calculated nine overlapping transitions (310, 317, 327, 348, 376, 404, 437, 465, and 497 nm) that produced the observed broad peak. For other conjugated materials in general, this result has been predicted by Jahn-Teller theory and reflected in the difficulty of maintaining planar structures—poor overlap of p_z orbitals.[47] These factors would explain high conversion to PPV while the UV spectra indicate that delocalization is apparently present over just a few repeat units.

VII. Multilayer Formation

Some solvation of polymer chains is evidenced by the irregular dewetting of the subphase during trough cleaning. However, it was confirmed that multilayer formation is the predominant process responsible for creep. X-ray diffractometer plots of one deposition samples yield approximately the same interference peak for vertical and horizontal deposition (see figure 15). Peak positions vary slightly. The peak of the vertically deposited sample is at $2\theta = 2.5°$ which corresponds to a spacing of 35.34 Å while that of the horizontally deposited sample is at $2\theta = 2.55°$ which corresponds to 34.63 Å. Both samples were made after allowing the film to creep to approximately one-eleventh of the starting area. The similarity in peaks indicates that essentially the same amount of material is deposited in both modes.

In another experiment, vertical deposition was carried out at different stages of creep (see figure 16 and table 3). One deposition was carried out almost immediately after reaching 25 mN/m (-4.2% of the original area). A second sample was prepared later in the creep process (-51.2% of the original area). To calculate an approximate ratio of scattering sites, the area beneath each of the curves was estimated by subtracting an approximate baseline and employing the trapezoidal approximation. The approximate ratio of scattering sites is $\frac{early}{late} = \frac{1}{2.4}$. Ideally, the site ratio should be $\frac{1}{2.9}$ for a film creeping at -5% / hour. The fair agreement shows that side chain order is maintained even after substantial amounts of creep.

UV - visible absorbance spectra also support this data. A plot of UV - visible absorbance shows a near linear relationship with the absorbance peak at 196 nm and the number of depositions (see figure 17 and table 3). Estimated absorbance (normalized to first layer) for a film creeping at -5% / hour is indicated by the solid line. Plotting the difference, however, shows the expected deviation from linearity (see figure 18 and table 4). The measured and calculated differences show good agreement.

In short, the results of these experiments are conclusive proof that multilayers form at the air-water interface. Multilayer formation brings into question the usefulness of the creep compensated transfer ratio as a quantitative calculation. Qualitatively, the creep compensated transfer ratio still may be used to determine the mode of deposition.

IX. Brewster Angle Microscopy

Preliminary work in Brewster angle microscopy gave blank images suggesting that the PPV films are either totally amorphous or that the crystallite sizes are smaller than the resolution of the BAM technique. This was shown to be true for pressures from 10.4 mN/m up to the collapse pressure of 46 mN/m. Qualitatively, images of the film from 10.4 to 46 mN/m appear to be identical (see figure 19a). Near the top of the image, there is a lighter region. This is due to a slight misalignment of the BAM optics and the inherently unequal illumination of the laser source (a Gaussian distribution of intensity around the center of the beam).

Figure 20 is a histogram of pixel intensity for BAM images of the same PPV films. The histogram of the 480×640 images (307200 pixels) were exactly the same for films at 10.4, 15.3, and 46 mN/m. There are several possible explanations for this result. First, crystallites are present and their sizes are smaller than the resolution of the BAM ($\sim 1\ \mu m$). Second, the film is isotropic in the plane of the air-water interface. Third, the refractive index of the film and the water surface are closely matched allowing the majority of the light that hits the film to pass through instead of being reflected to the camera. For stretched bulk films, PPV has been measured to have an index of refraction of 2.1 ± 0.2 parallel to orientation and a value of 1.5 ± 0.2 perpendicular to orientation.[48] As a point of comparison, the histogram of a particularly dusty portion of the film is included to demonstrate the difference in the resolution of the BAM when the laser hits anisotropic objects (see figure 19b). The contrast was enhanced using a function built into Aldus Photostyler, however the histogram was taken of an unenhanced image. Image reproduction is poor and not representative of the image observed on the computer monitor.

X. Polymer Film Doping

$FeCl_3$ was chosen for its stability and ease in handling. In the studies previously mentioned, SO_3 has been reported to dedope slowly with time and AsF_5 was found to be unstable in the presence of water and air.[49,50] Like other dopants $FeCl_3$ tends to turn PPV films opaque, a property we wish to avoid in LC alignment layer design. However, if the film is thin enough, display properties should not be greatly affect.

Spectra taken of the doped films showed dramatic changes. Figure 21 shows that wavelengths across the visible range (450 - 640 nm) are uniformly absorbed or reflected by the film. The peak absorbance at 200 nm corresponding to the $\Pi - \Pi^*$ transition of the phenyl ring appears to be unaffected while the absorption centered about 390 nm is no longer observed. The IR spectrum (figure 22) shows only broad absorbances rising at 4000 cm^{-1} sloping down to another broad peak centered about 3400 cm^{-1}. A small broad peak is also visible at approximately 650 cm^{-1}. A single well-defined peak 1595.15 cm^{-1} probably corresponds to the vibrational mode associated with 1,4 substituted benzene.

In a $FeCl_3$ doping study of poly (p-phenylene sulfide) (PPS), Piaggio interpreted a similar spectra as corresponding to metallic behavior.[51] Using an analogous interpretation for $FeCl_3$ doped PPV, the rising absorption near the high frequency end corresponds to the tail of the subgap electronic absorption in the visible which extends to the near infrared. The rise near the fingerprint region is due to increased reflectivity caused by an increase in the index of refraction. This behavior is characteristic of metallic behavior.

XI. Conductivity Measurements

Preliminary conductance measurements from 5 deposition samples of the precursor, PPV, and $FeCl_3$ doped PPV gave results below $10^{-10}(\Omega)^{-1}$. This is the estimated lowest sensitivity of the instrument. Thicker samples were not attempted since delamination has been observed to occur after 5 depositions. Since layer thicknesses were not known, a conductivity could not be calculated. Determination of layer thicknesses will be required for future work.

XII. Liquid Crystal Cells

PPV was observed to produce liquid crystal alignment for samples of 5 depositions. Samples prepared with less than 5 depositions gave only localized alignment and had

more defects. The converted polymer gave better alignment subjectively seen as darker extinction (45°) and brighter transmission (0°) when place between cross polarizers. Some macroscopic defects were seen as streaks perpendicular to dipping direction and as disordered domains. Twisted nematic LC cells were made with some success although macroscopic defects were easily visible to the eye. Further work is required.

Conclusion

Poly (p-xylene-α-diethyl sulphonium perfluorononanoate) was found to creep at 25 mN/m at 13°C. Multilayer formation was determined to be the mechanism by which creep occurred as shown by UV-vis spectroscopy and X-ray. Deposition of these multilayers was found to be Z-type. However, after 3 iterations an irregular deposition / delamination process was observed.

IR absorbance spectroscopy found almost complete thermal elimination of the side chain and conversion to PPV at 1 kPa and 235°C. UV-vis spectroscopy results are consistent with Karasz's hypothesis—the lowest energy absorbance probably corresponds to an energy transition other than the effect of completely conjugated PPV. Doping of these thin films gave results consistent with metallic behavior. Lastly, construction of LC cells using these films as alignment layers was successful for samples of 5 layers. Work continues in further characterization of these films.

Acknowledgment

This work was supported by the Office of Naval Research under grant N00014-94-1-0270.

References

[1]Chen, D., Winokur, M, Masse, M., Karasz, F. (1990) *Phys. Rev. B* **41** (10), 6759.

[2]Hiltrop, K., Stegemyer, H., *Liquid Crystals and Ordered Fluids*, vol. 4; (1983) Plenum Press, New York, p. 515.

[3]Morozumi, S. "Materials and Assembling Process of LCD's", *Liquid Crystals: Applications and Uses*, Vol I; Bahadur, B., ed.; (1990) World Scientific, Singapore, p. 184.

[4]Morozumi, S. "Materials and Assembling Process of LCD's", *Liquid Crystals: Applications and Uses*, Vol I; Bahadur, B., ed.; (1990) World Scientific, Singapore, p. 185.

[5]Roberts, G. *Langmuir - Blodgett Films* (1990) Plenum Press, New York, p. 338.

[6]Bradley, D., Brown, A., Burn, P., Burroughes, J., Friend, R., Holmes, A., Mackay, K., Marks, R. (1991) *Synth. Met.* **41-43**, 3135.

[7]Katz, H., Bent, S., Wilson, W., Schilling, M., Ungashe, S., (1994) *J. Am. Chem. Soc.* **116**, 6631.

[8]Colaneri, N., Bradley, D., Friend, R., Burn, P., Holmes, A., Spangler, C., (1990) *Phys. Rev. B,* **42** (18), 11670.

[9]Katz, H., Bent, S., Wilson, W., Schilling, M., Ungashe, S., (1994) *J. Am. Chem. Soc.*, **116**, 6631.

[10]Yu, J., Hsu, J., Chuang, K., Chao, C., Chen, S., Kao, F., Fann, W., Lin, S., (1995) *Synth. Met.*, **74**, 7.

[11]Lefrant, S., Perkin, E., Buisson, J., *Synth. Met.* (1989), **29**, E91.

[12]Bradley, D., Friend, R., Lindenberger, H., Roth, S. (1986) *Polymer,* **27**, 1709.

[13]Tian, B., Zerbi, G., Müllen, K. (1991) *J. Chem. Phys.* **95** (5), 3198.

[14]Tian, B., Zerbi, G., Müllen, K. (1991) *J. Chem. Phys.* **95** (5), 3191.

[15]Woo, H., Lhost, O., Graham, S., Bradley, D., Friend, R., Quattrocchi, C., Brédas.,Schenk, R., Müllen, K., (1993) *Synth. Met.* **59**, 13.

[16]Orbzut, J., Karasz, F., (1987) *J. Chem. Phys.* **87** (4), 2349.

[17]Orbzut, J., Karasz, F., (1987) *J. Chem. Phys.* **87** (4), 2349.

[18]Ohlemacher, A., Schenk, R., Weitze, H., Tyutyulkov, N., Tasseva, M., (1992) *Makromol. Chem.* **193**, 81

[19]Dretahl, Y., Kühmstedt, R., Oswald, H., Hörhold, H., (1970) *DieMakrom. Chemie*, **131**, 89.

[20]Yank, J., Greiner, A., Bässler, H., Bradley, D., (1990) *Makromol. Chem., Rapid Commun.*, **11**, 415.

[21]Tian, B., Zerbi, G., Schenk, R.; Müllen, K., (1991) *J. Chem. Phys.* **95**, (5), 3191.

[22]Bradley, D., (1987) *PhD Thesis* University of Cambridge, UK.

[23]Bradley, D., Evans, G., Friend, R., (1987) *Synth. Met.*, **17**, 651.

[24]Capistran, J., Gagnon, D., Antoun, S., Lenz, R., Karasz, F., (1984) *ACS Polym. Preprints* **25**, 282.

[25]Nishikata, Y.; Kakimoto, M. J. Chem. Soc., Chem. Commun. 1988, 1040.

[26]Lefrant, S., Perrin, E., Buisson, J.P., *Synth. Met.*\(1989) **29**, E91.

[27]Zhang, X., Tendeloo, G., Landuyt, J., Dijck, D., Briers, J., Bao, Y., Geise, H., (1996) *Macromolecules*, **29**, 1554.

[28]Kim, J., Kim, Y., Sohn, B., Kang, D., Jin, J., Kim, C., Pyun, C., *Synth. Met.* (1995) **71**, 2023.

[29]Halliday, D., Burn, P., Friend, R., Holmes, A. *J. Chem. Soc., Chem. Commun.*, (1992) 1685.

[30]Y. Nishikata, Kakimoto, M., Imai, Y. *J. Chem. Soc., Chem. Commun.* (1988), 1040.

[31]Chen, D., Winokur, M, Masse, M., Karasz, F. (1990) *Phys. Rev. B* **41** (10), 6759.

[32]Karasz, F., Capistran, J., Gagnon, D., Lenz, R., (1985) *Mol. Cryst. Liq. Cryst.* **118**, 327.

[33]Wessling, R.; Zimmerman, R., U.S. Pat. 3,401,152.

[34]Wessling, R.; Zimmerman, R., U.S. Pat. 3,706,677.

[35]Halliday, D.; Burn, P.L.; Friend, R.H.; Holmes, A.B., (1992) *J. Chem. Soc. Chem. Commun.*, 1685.

[36]Gagnon, D.; Capistran, J.; Karasz, F.; Lenz, R.; Antoun S., (1987) *Polymer* , **28**, 567.

[37]Nishikata, Y.; Kakimoto, M. (1988) *J. Chem. Soc., Chem. Commun.*, 1040.

[38]Murase, I., Ohnishi, T., Noguchi, T., Hirooka, M. (1984) *Polym. Commun.* **25**, 327.

[39]Piaggio, P., Musso, G., Dellepiane, G., (1995) *J. Phys. Chem.* **99**, 4187.

[40]Gagnon, D.; Capistran, J.; Karasz, F.; Lenz, R.; Antoun S., (1987) *Polymer* , **28**, 567.

[41]Gagnon, D.; Capistran, J.; Karasz, F.; Lenz, R.; Antoun S., (1987) *Polymer* , **28**, 567

[42]Woo, H.; Lhost, O.; Graham, S.; Bradley, D.; Friend, R.; Quattrocchi, C.; Brédas, J.; Schenk, R.; Müllen, K., (1993) *Synth. Met.*, **59**, 13.

[43]Murase, I., Ohnishi, T., Noguchi, T., Hirooka, M. (1984) *Polym. Commun.* **25**, 327.

[44]Nishikata, Y.; Kakimoto, M. (1988) *J. Chem. Soc., Chem. Commun.*, 1040.

[45]Woo, H., Lhost, O., Graham, S., Bradley, D., Friend, R., Quattrocchi, C., Brédas.,Schenk, R., Müllen, K., (1993) *Synth. Met.* **59**, 13.

[46]Orbzut, J., Karasz, F., (1987) *J. Chem. Phys.* **87** (4), 2349.

[47]Blythe, A. *Electrical Properties of Polymers* (1979) Cambridge University Press, Cambridge, p. 105.

[48]Bradley, D., (1987) *Phys. D: Appl. Phys* **20**,1389.

[49]Nishikata, Y.; Kakimoto, M. (1988) *J. Chem. Soc., Chem. Commun.*, 1040.

[50]Wnek, G.; Chien, J.; Karasz, F.; Lilya, C., (1979) *Polymer*, **20**, 1441.

[51]Piaggio, P., Musso, G., Dellepiane, G., (1995) *J. Phys. Chem.* **99**, 4187.

PRECURSOR				
wavenumber	**absorbance**	**relative**	**Assignment**	**Reference**
(1/cm)	(a.u.)	**strength**		
3232.1	0.0061	m	water	
2918.6	0.0065	m	CH_2 stretch	G(p. 13)
2850.1	0.0053	w	CH (tertiary)	G(p. 13)
1781.4	0.0073	m	COO^- stretch	I
1685.0	0.0149	s	C=O stretch	F, G(p. 162)
1611.7	0.0053	w	quadrant ring stretch	D, E
1515.2	0.0048	w	semicircle ring stretch	B,D
1365.7	0.0055	w	CH_2 stretch C-F, $CF-CF_3$ grouping	I G (p. 329)
1204.6	0.0258	vs	C-F mode	F,G (p. 329)
1148.7	0.0199	s	C-F mode	G (p. 329)
1115.9	0.0084	m	C-F mode	G (p. 329)
1062.9	0.0067	m	C-O stretch	I
982.9	0.0060	m	trans $CH-CH_2$ stretch	G
795.7	0.0064	m	$CF-CF_3$ grouping	G (p. 329)
724.4	0.0071	m	$CF-CF_3$ grouping	G (p. 329)
663.6	0.0065	m	RCH_2-S- stretch	G (p. 354)
560.4	0.0070	m	p-phenylene out of plane ring bend	D(555 1/cm) E (555 1/cm)
502.5	0.0191	vs	C-F bend	I

A Lefrant, S.; Permin, E.; Buisson, J., *Synth. Met.* 29 (1989) E91.
B Tian, B.; Zerbi, G.; Müllen, K., *J. Chem. Phys.*95 (55), 1 (1991) 3198.
D Bradley, D.; *J. Phys. D. Appl. Phys.* 20 (1987) 1389.
E Bradley, D.; Friend, R.; Lindenberger, H.; Roth, S.;*Polymer* 27 (1986) 1709.
F Nishikata, Y.; Kakimoto, M.; Imai, Y., *Mol. Cryst. Liq. Cryst.*
G L. J. Bellamy *The Infrared Spectra of Complex Molecules* (2nd ed.) (1966). New York: Wiley and Sons.
H N. Colthup, L. Daley, S. Wiberley *Introduction to Infra-red and Raman Spectroscopy* (1964) New York: Academic Press
I Koenig, J., personal communication.

Table 1 IR peak absorbance assigments for the PPV - precursor

HEATED				
wavenumber (1/cm)	absorbance (a.u.)	relative strength	Assignment	Reference
3347.3	0.0010	w	water	
3025.1	0.0015	m	trans-vinylene CH stretch	B, D, E
1695.8	0.0016	m	C=O	
1599.3	0.0022	s	quadrant ring stretch (imperfection)	D, E
1516.4	0.0023	s	semi-circle ring stretch	B, D, E
1419.9	0.0014	m	semi-circle ring stretch	B, D
1171.0	0.0015	m	p-phenylene CH in-plane bend	B, D, E
1076.5	0.0014	m	p-phenylene CH in-plane bend	D
964.6	0.0030	s	trans-vinylene CH out of plane bend	C, D, E
837.3	0.0024	m	p-phenylene CH out of plane bend	D,.E
769.8	0.0009	w	C-C stretch and ring deformation	B
648.2	0.0011	m	?	
547.9	0.0022	m	p-phenylene out of plane ring bend?	D(555 1/cm) E(555 1/cm)
503.5	0.0029	s	?	

A Lefrant, S.; Permin, E.; Buisson, J., *Synth. Met.* 29 (1989) E91.
B Tian, B.; Zerbi, G.; Müllen, K., *J. Chem. Phys.*95 (55), 1 (1991) 3198.
D Bradley, D.; *J. Phys. D. Appl. Phys.* 20 (1987) 1389.
E Bradley, D.; Friend, R.; Lindenberger, H.; Roth, S.;*Polymer* 27 (1986) 1709.
F Nishikata, Y.; Kakimoto, M.; Imai, Y., *Mol. Cryst. Liq. Cryst.*
G L. J. Bellamy *The Infrared Spectra of Complex Molecules* (2nd ed.) (1966). New York: Wiley and Sons.
H N. Colthup, L. Daley, S. Wiberley *Introduction to Infra-red and Raman Spectroscopy* (1964) New York: Academic Press
I Koenig, J., personal communication.

Table 2 IR peak absorbance for the precursor after being heated at 235°C for 7 hours

	estimated				measured	
$deposition_i$	$time_i$ (min)	$fract_i$	$absorbance_i$	$normalized_i$	$absorbance_i$	$normalized_i$
0	0.00	1.00	0.00	0.00	0.00	0.00
1	38.53	0.97	1.03	1.00	0.02	1.00
2	81.07	0.93	2.11	2.04	0.05	2.04
3	123.60	0.90	3.22	3.12	0.07	3.16
4	166.13	0.86	4.38	4.24	0.08	3.29

$$(\text{fraction}_i \text{ of area}_o) = 1 - (0.05 \times time_i)$$

$$\text{absorbance}_i \text{ (a.u.)} = \left(\sum_i \frac{1}{fract.area_i} \right) - 1$$

(the negative 1 term is used since no layer picked up on the first iteration)

is

$$\text{normalized absorbance}_i = \frac{absorbance_i}{absorbance_1}$$

38.53 minutes elapse before the first layer is deposited.

42.53 minutes elapse between subsequent depositions.

Table 3 Estimated absorbances for -5% / hour creeping film, measured absorbances, and the respective normalized values.

	estimated		measured	
deposition	normalized	residual	normalized	residual
0	0.00	0.00	0.00	0.00
1	1.03	0.00	1.00	0.00
2	2.11	0.04	2.04	0.04
3	3.22	0.12	3.16	0.16
4	4.38	0.24	3.29	-0.71

residual_i = normalized absorbance_i - interation_i

Error bars were calculated by propogating an RMS deviation of 0.001 at 196 nm for blank slides. This RMS deviation translates to $\pm$ 0.046 when normalized.

Table 4 Calculated deviation from linearity for the estimated and measured normalized absorbances

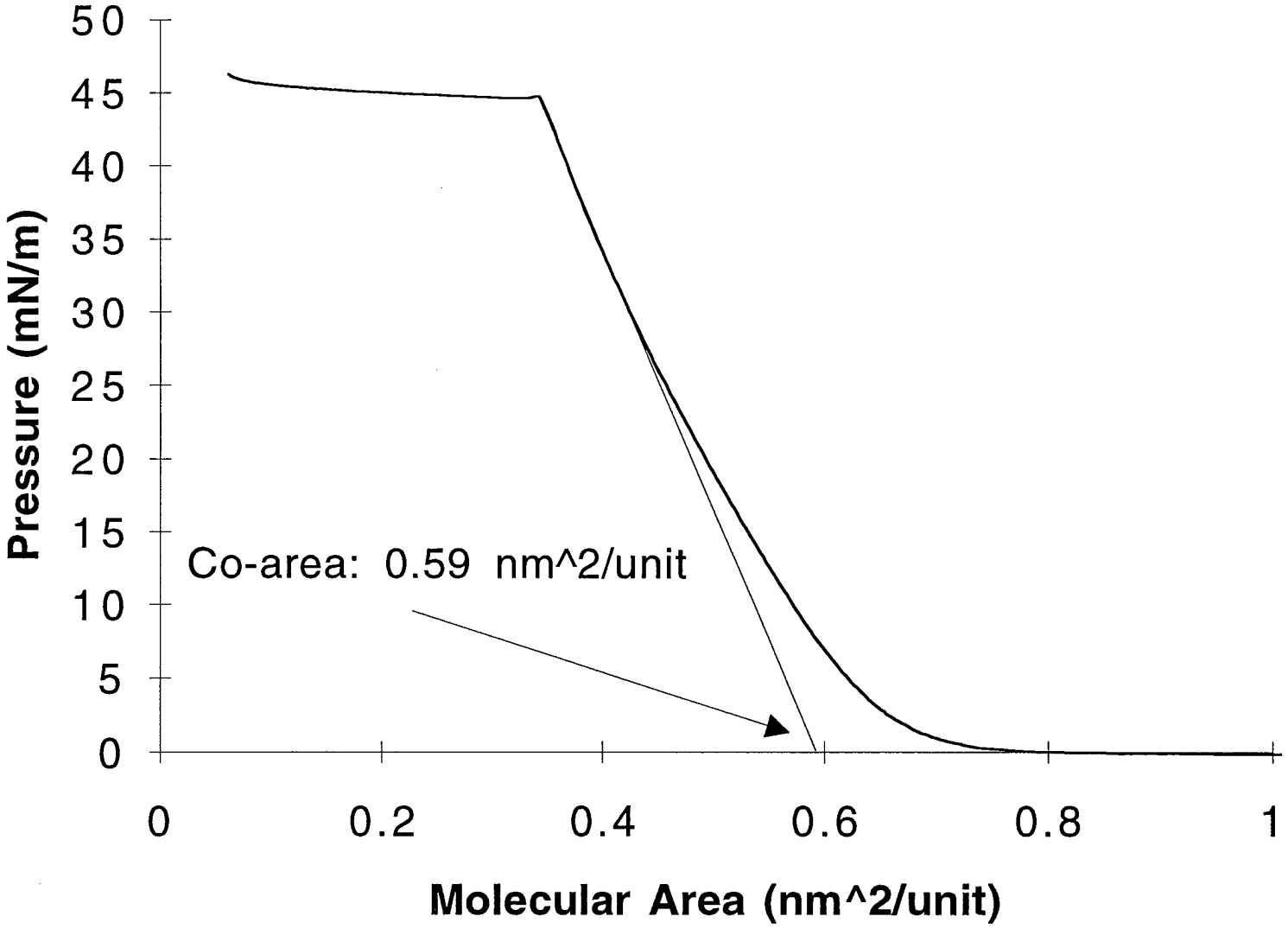

Figure 1 Surface pressure - area isotherm of the PPV precursor at 13.8°C.

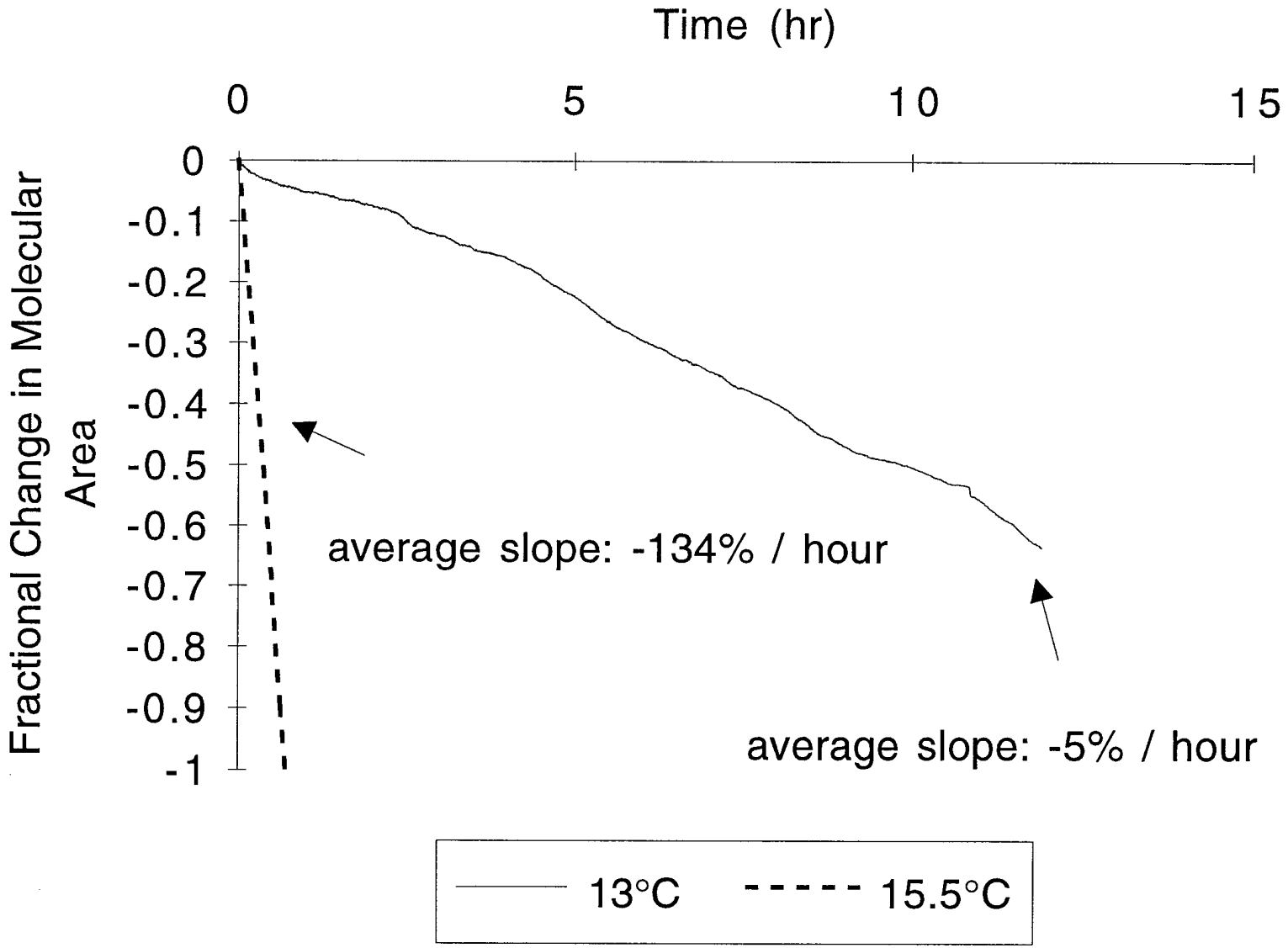

Figure 2 Compressive creep plot of fractional change in molecular area versus time for the PPV-Precursor at 25 mN/m.

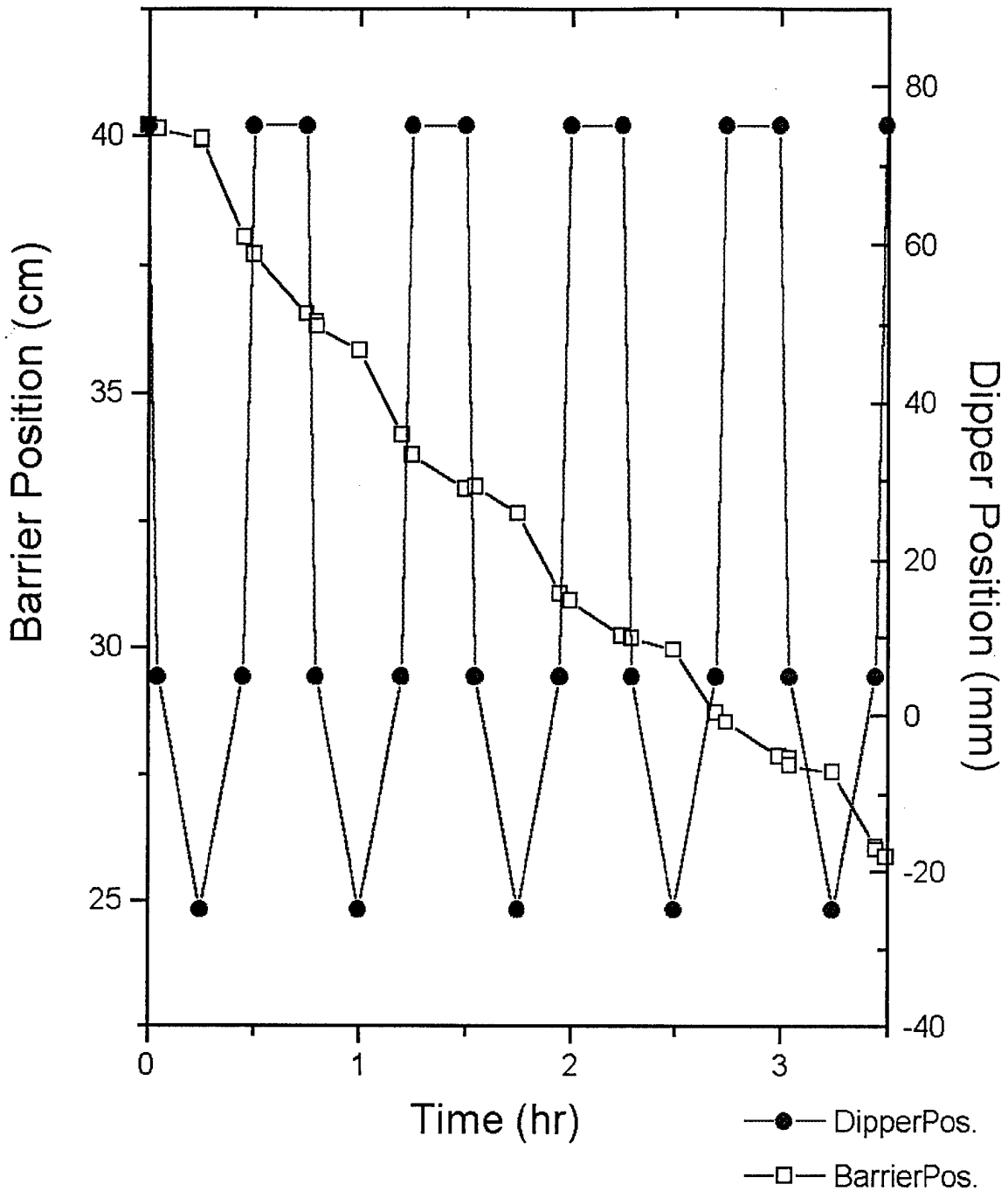

Figure 3 Dual plot of barrier and dipper position versus time for deposition onto glass at 25 mN/m and 8.4°C

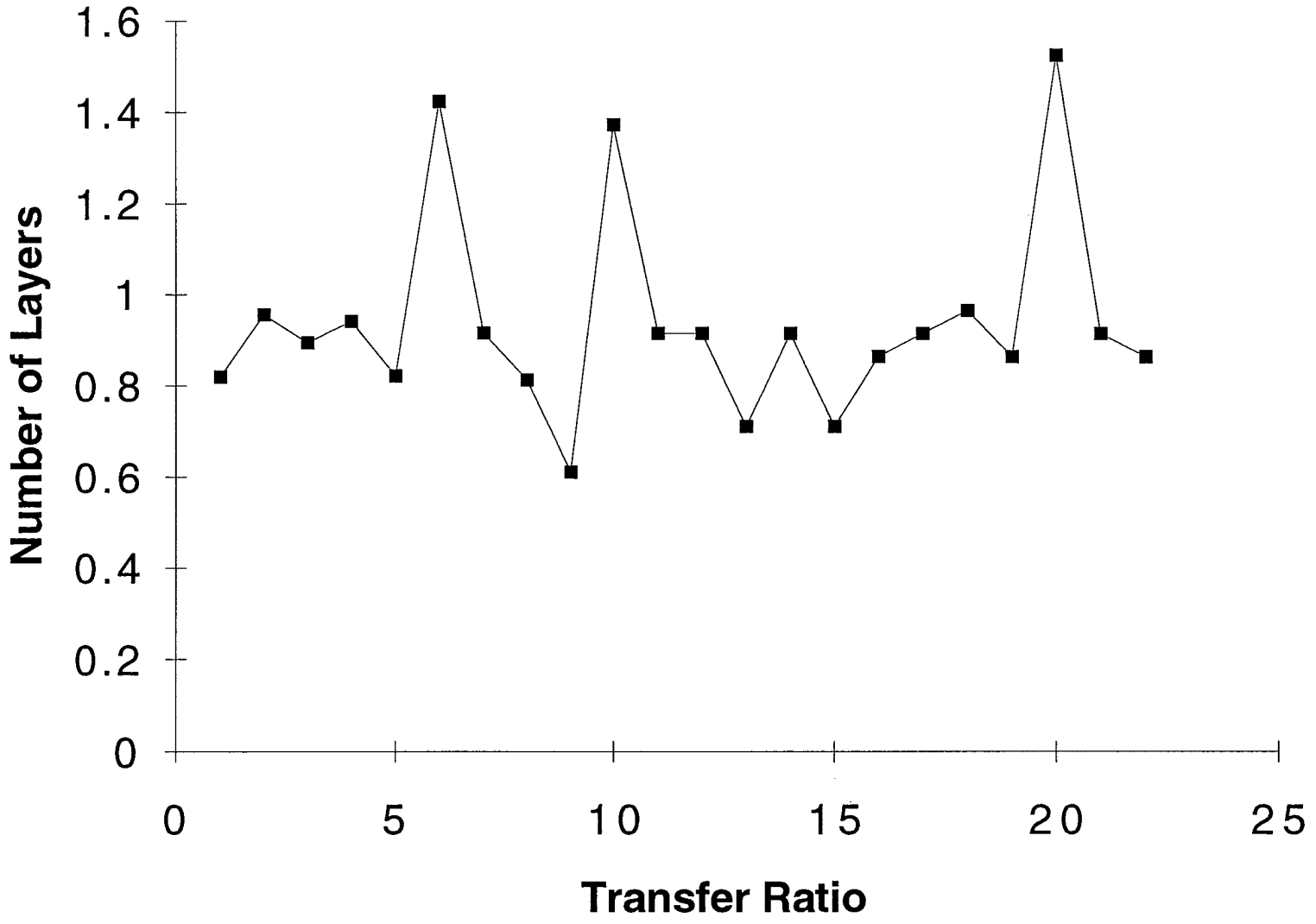

Figure 4 Plot of transfer ratio versus the number of layers for deposition of the PPV precursor onto a hydrophilic glass substrate

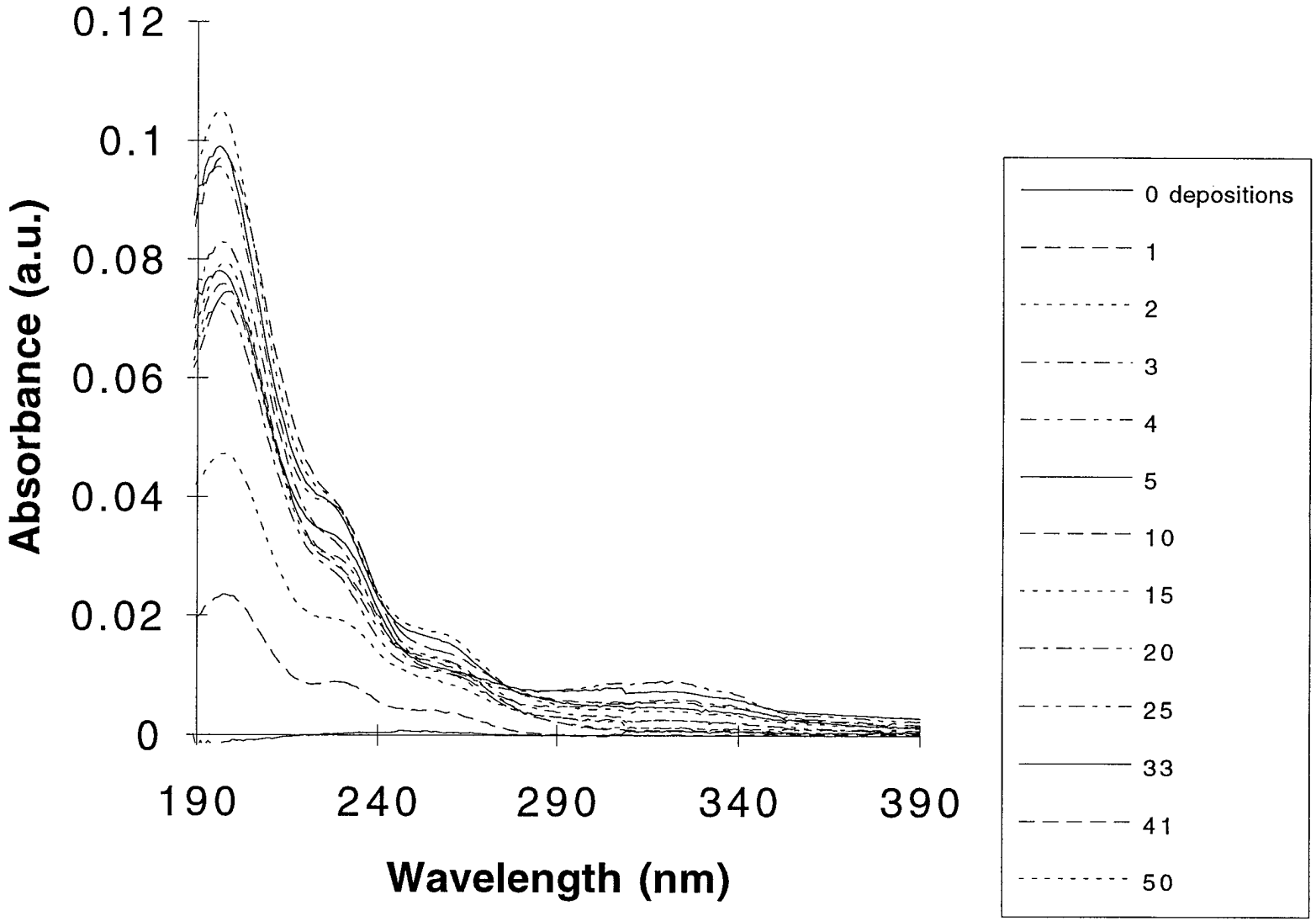

Figure 5 Plot of UV - visible absorbance for PPV - precursor samples after various numbers of depositions

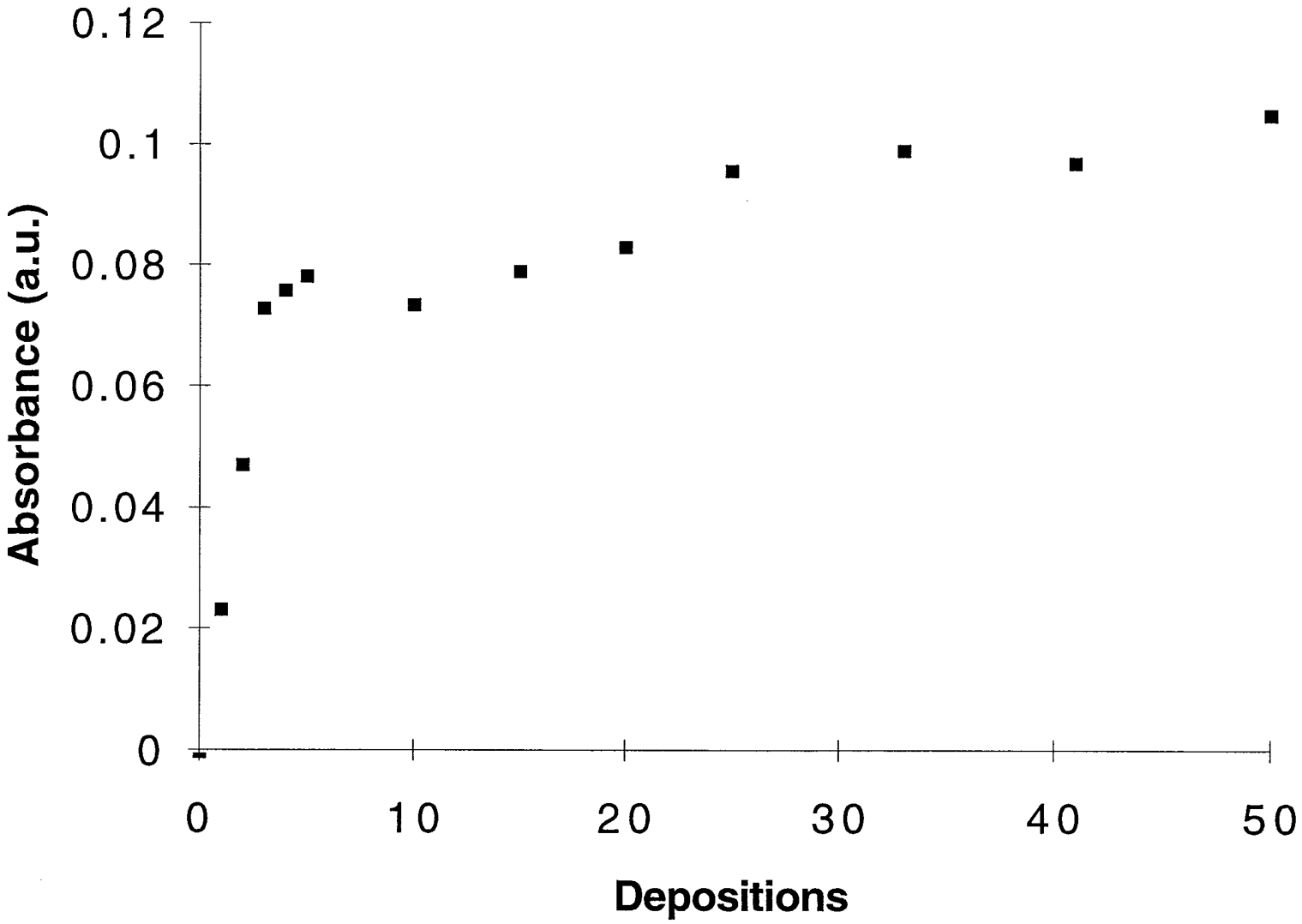

Figure 6 Plot of UV - visible absorbance at 196 nm versus the number of depositions for PPV - precursor samples of various thicknesses

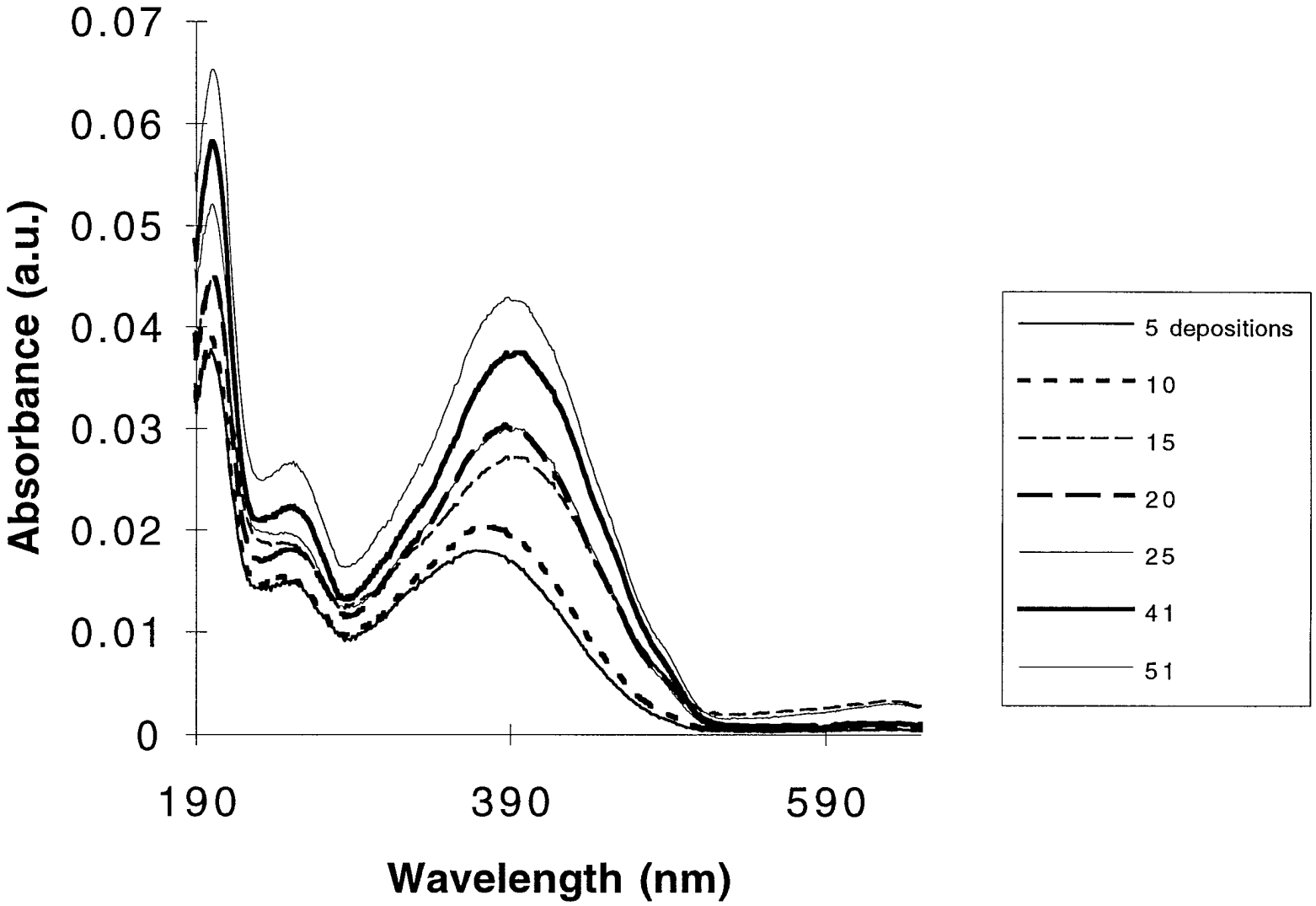

Figure 7 Plot of UV - visible absorbance for PPV - precursor samples of various thicknesses after heating at 235°C for 7 hours

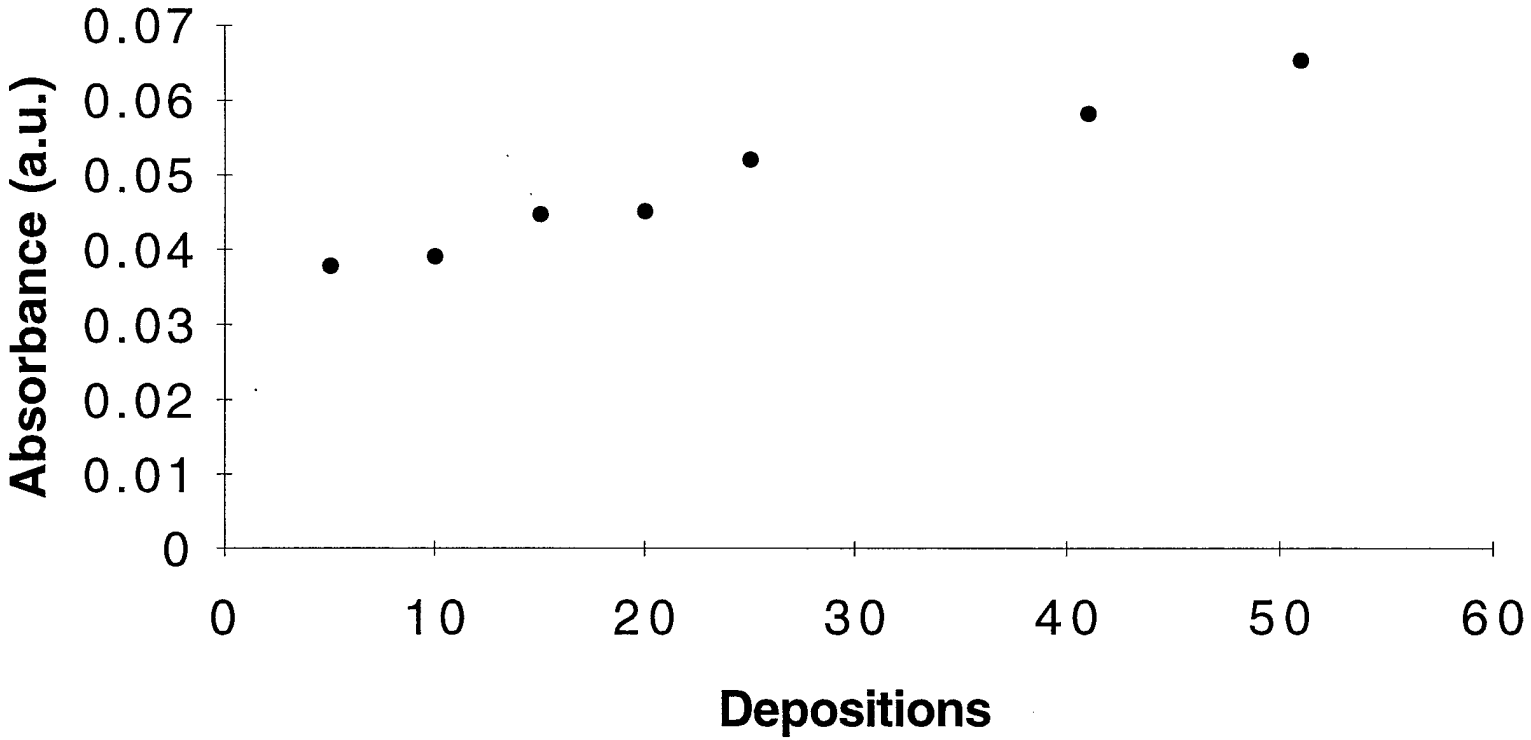

Figure 8 Plot of UV - visible absorbance at 200 nm versus the number of depositions for PPV - precursor samples of various thicknesses (235°C, 7 hours)

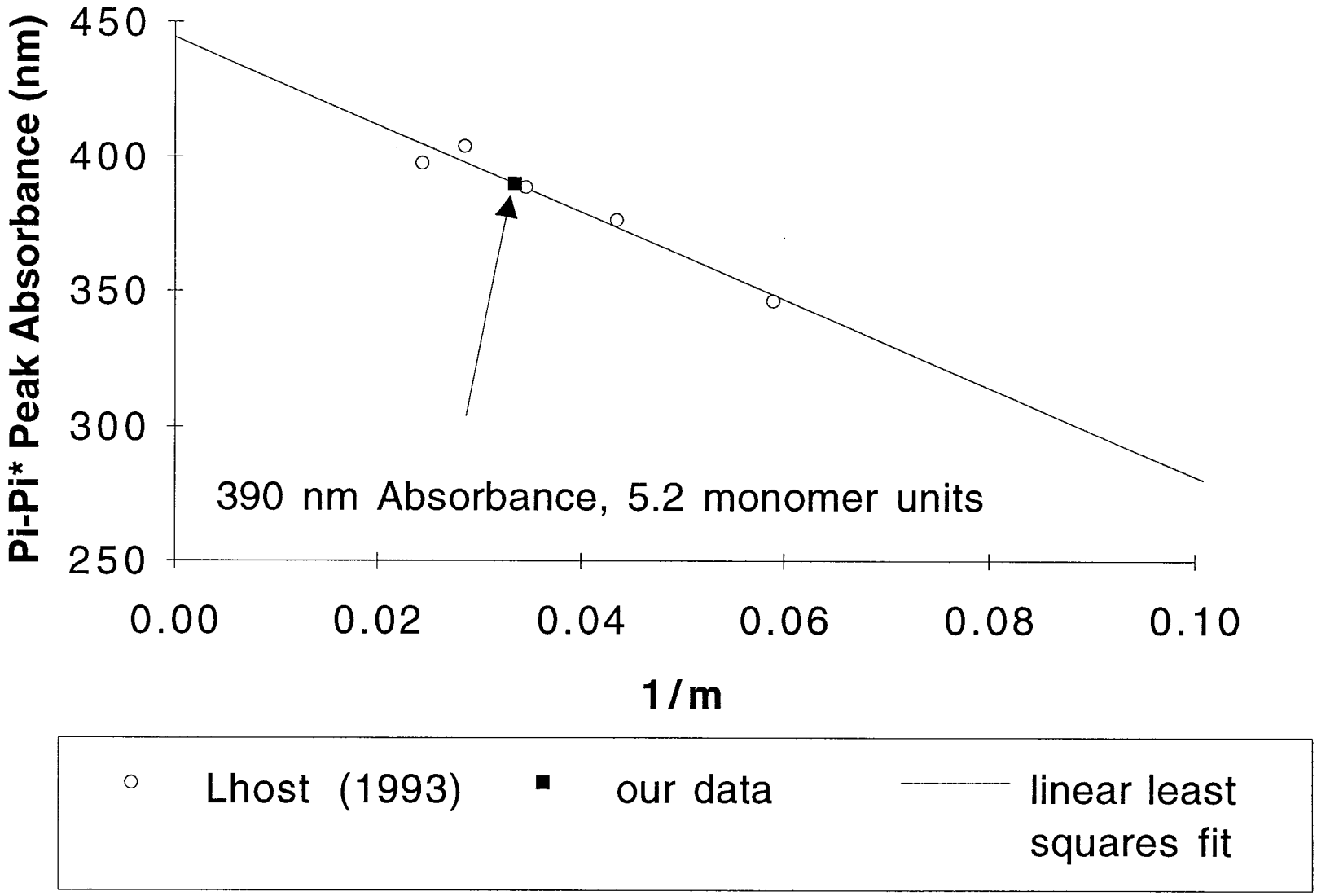

Figure 9 Plot of peak absorbance of the lowest UV-vis transition vs. 1/(conjugation length) for PPV oligomers of various lengths

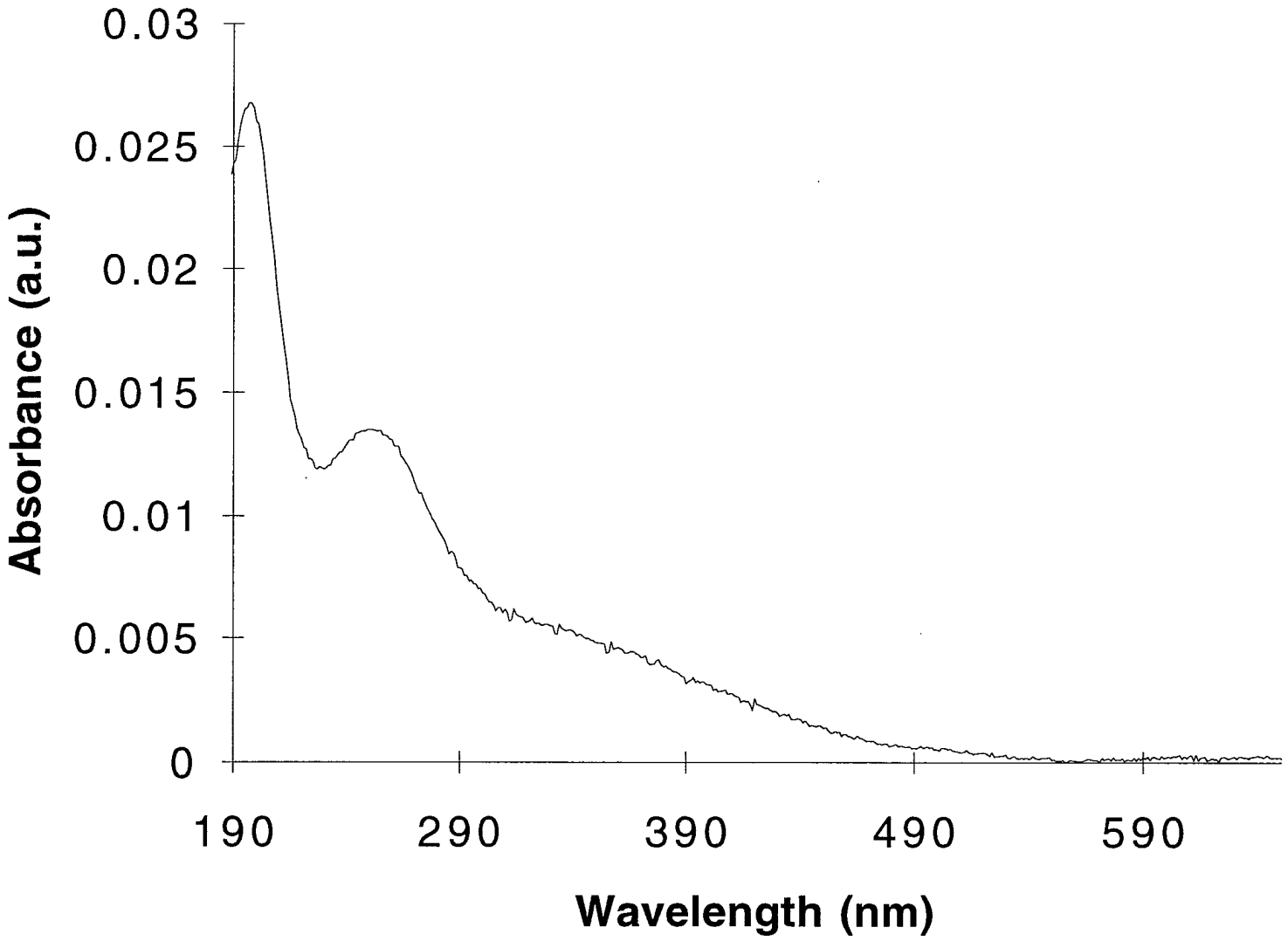

Figure 10 Plot of UV - visible absorbance for a PPV sample after being heated at 300°C for 7 hours

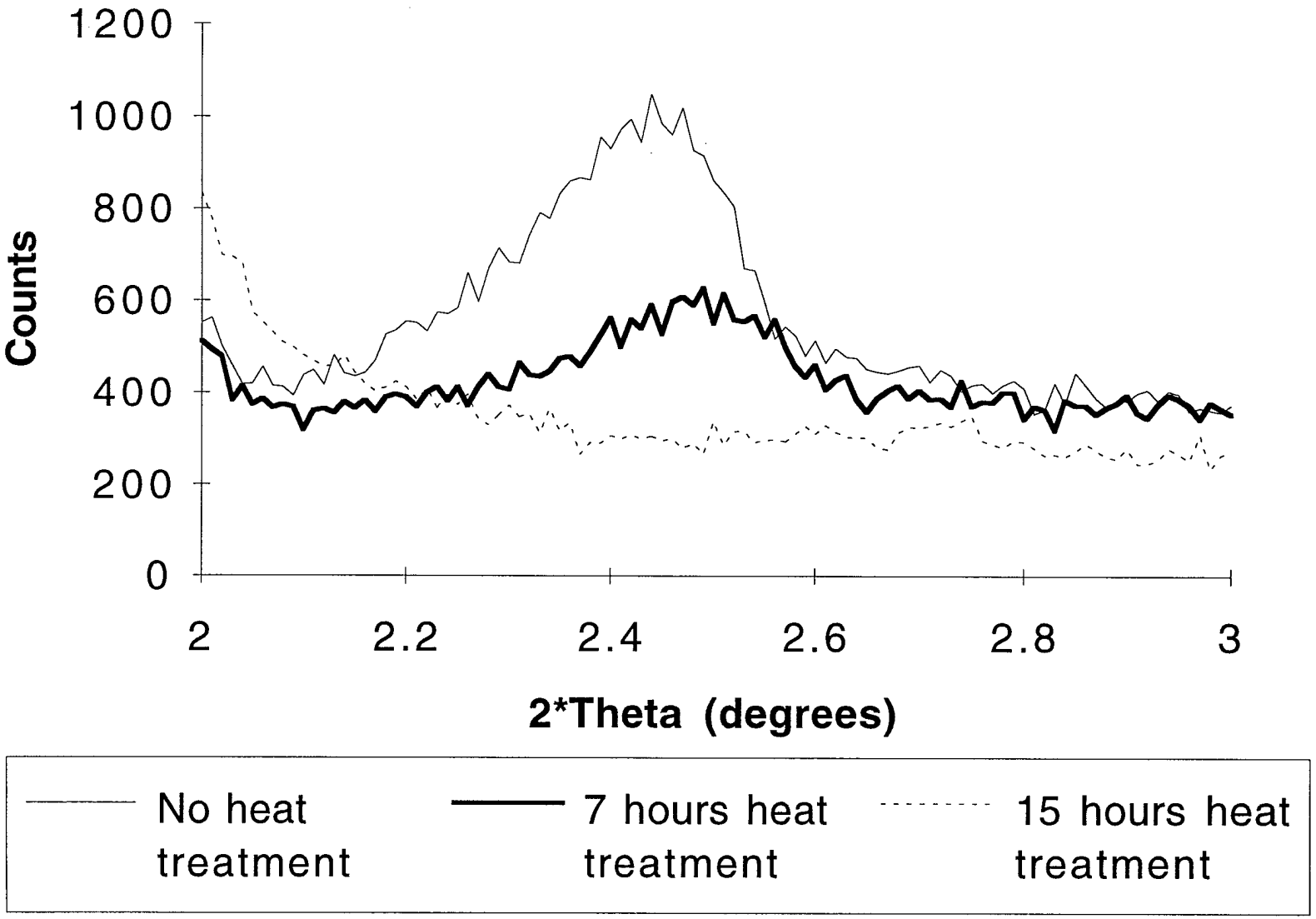

Figure 11 X-ray diffractometer plot of a 5 deposition sample before and after heat treatment

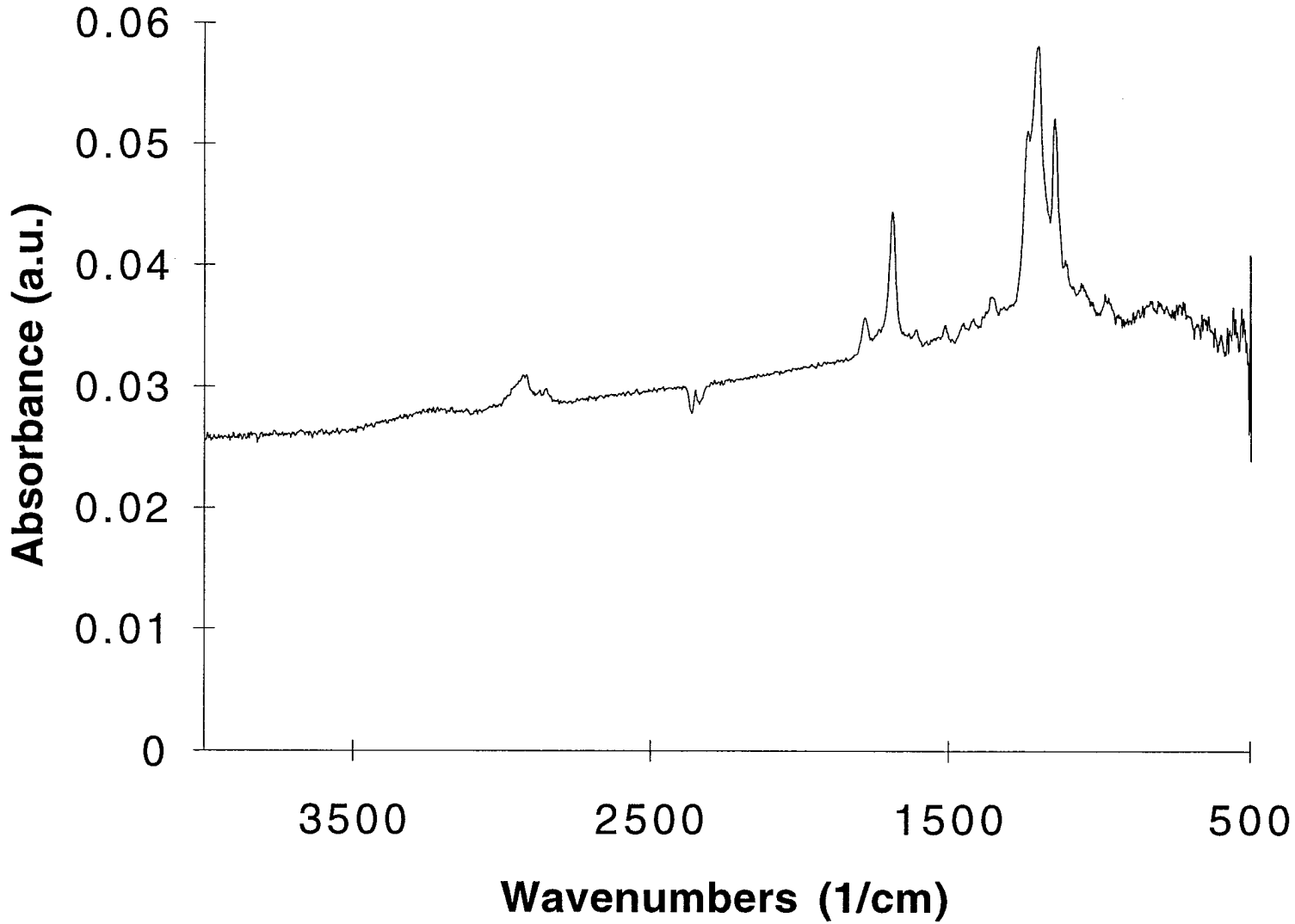

Figure 12 IR Absorbance spectra of the PPV precursor (100 depositions)

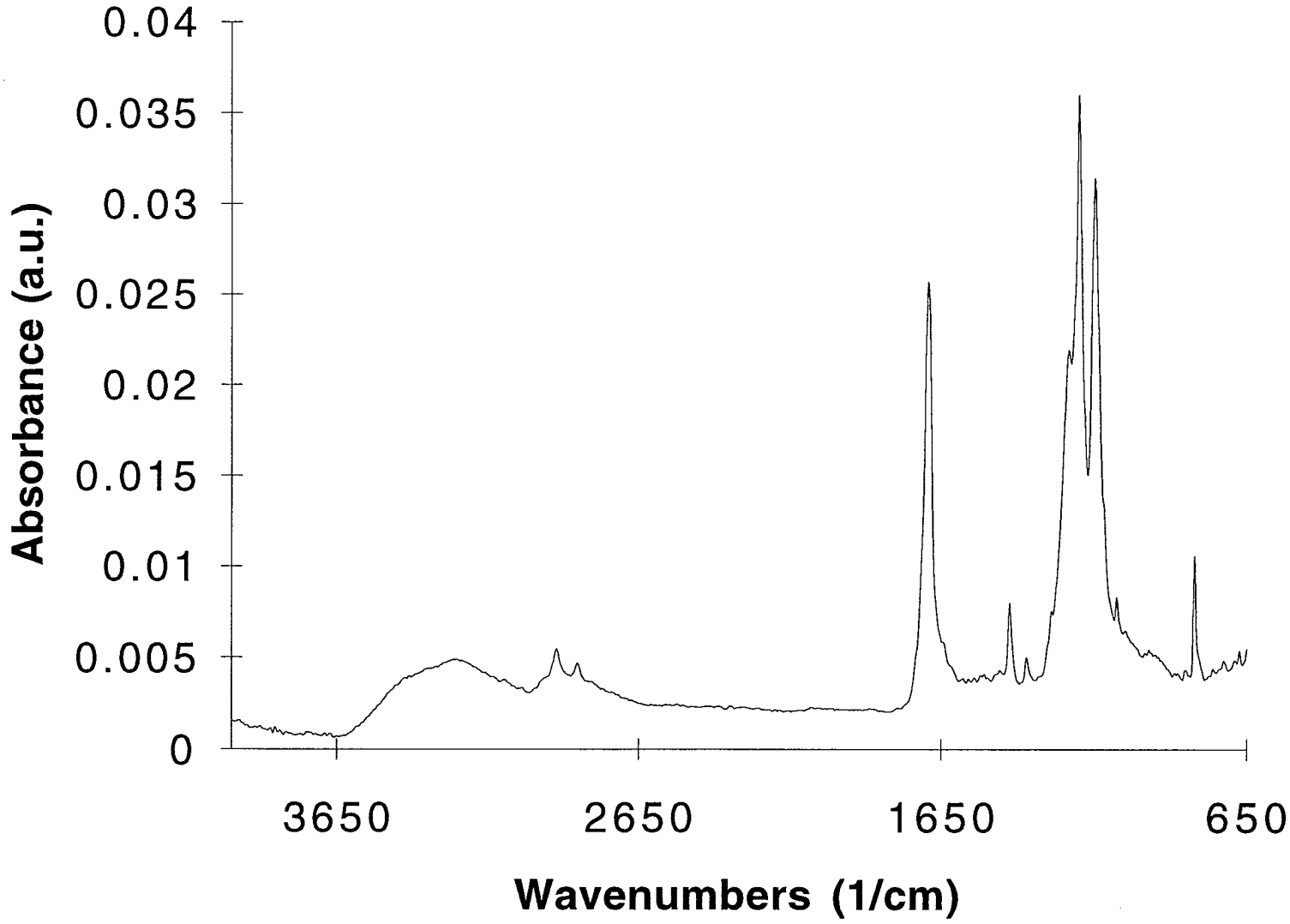

Figure 13 IR absorbance spectra of sodium perfluorononanoate

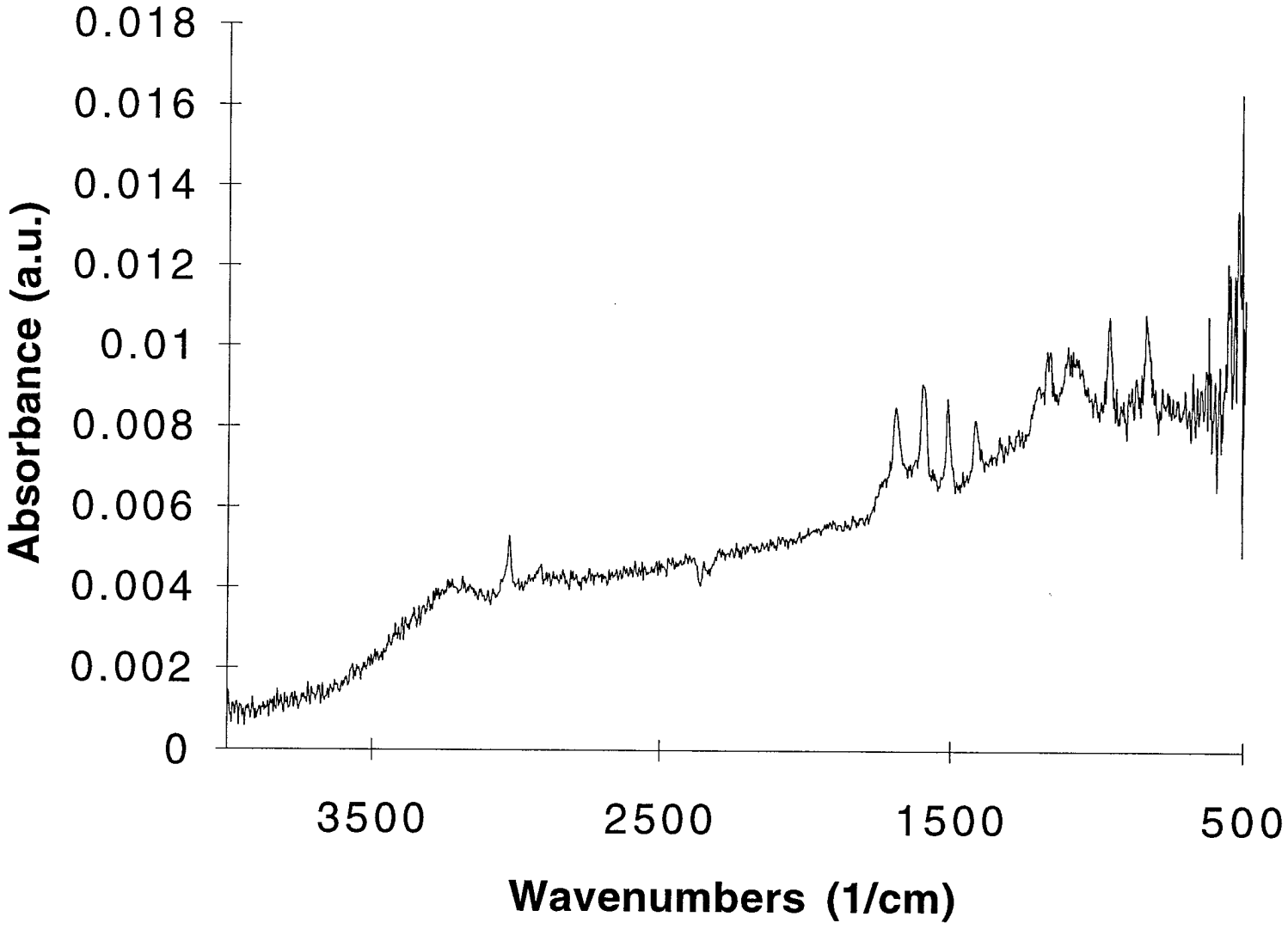

Figure 14 IR absorbance plot of the PPV precursor after heat treatment (7 hours, 235°C)

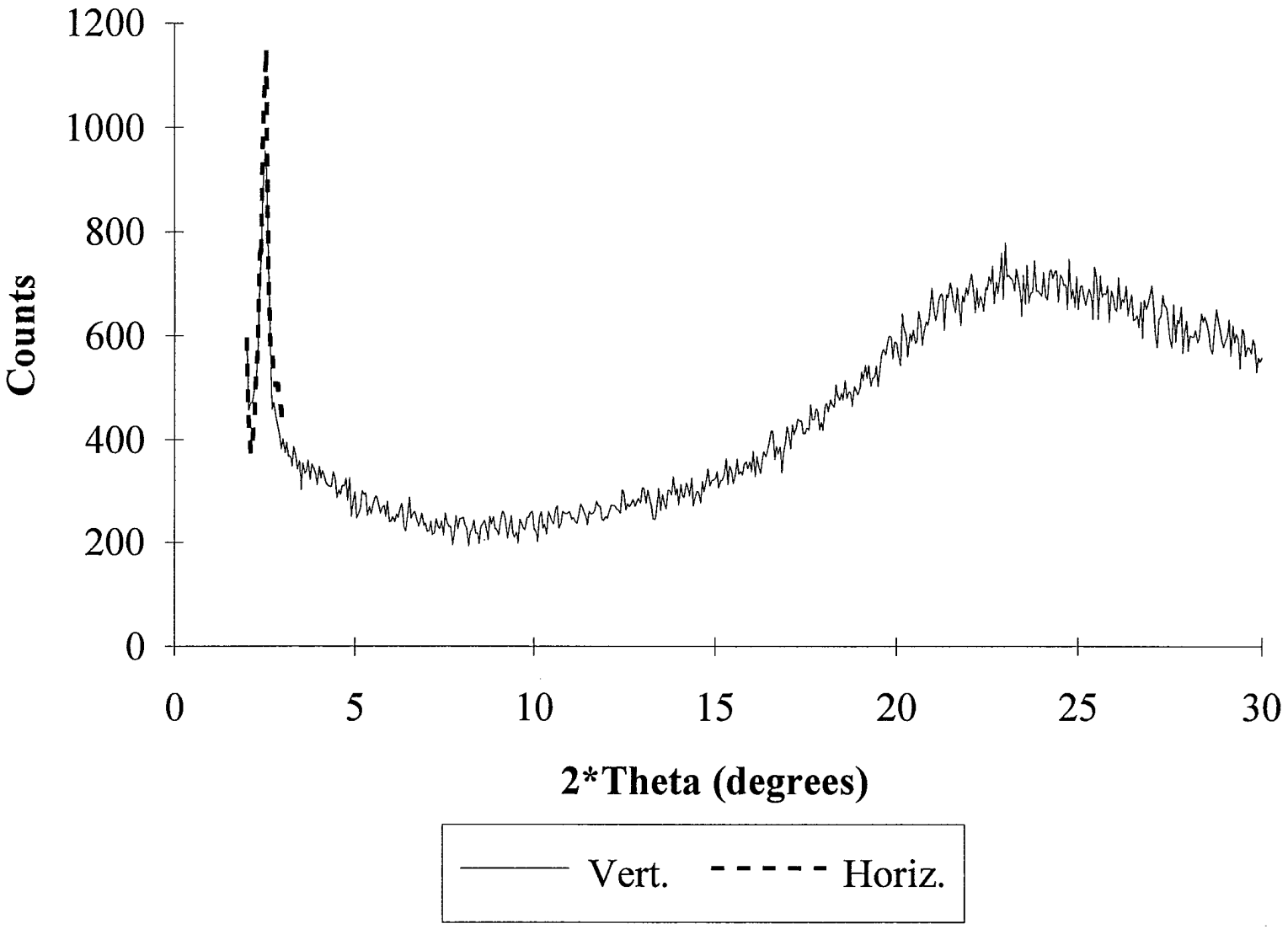

Figure 15 X-ray diffractometer plots of PPV - precursor samples after 1 deposition

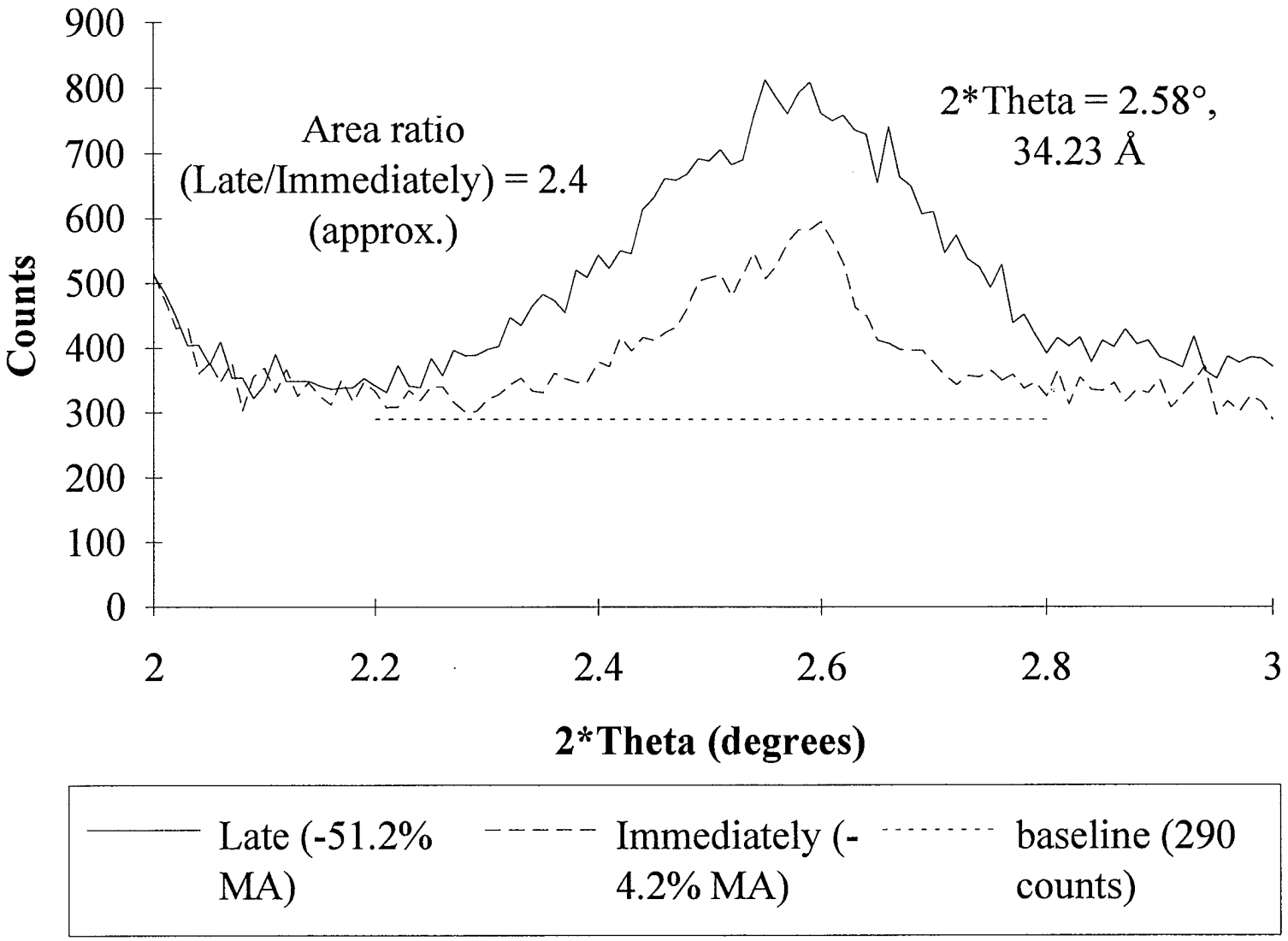

Figure 16 X-ray diffractometer plots for 1 deposition PPV - precursor samples prepared at various stages of creep

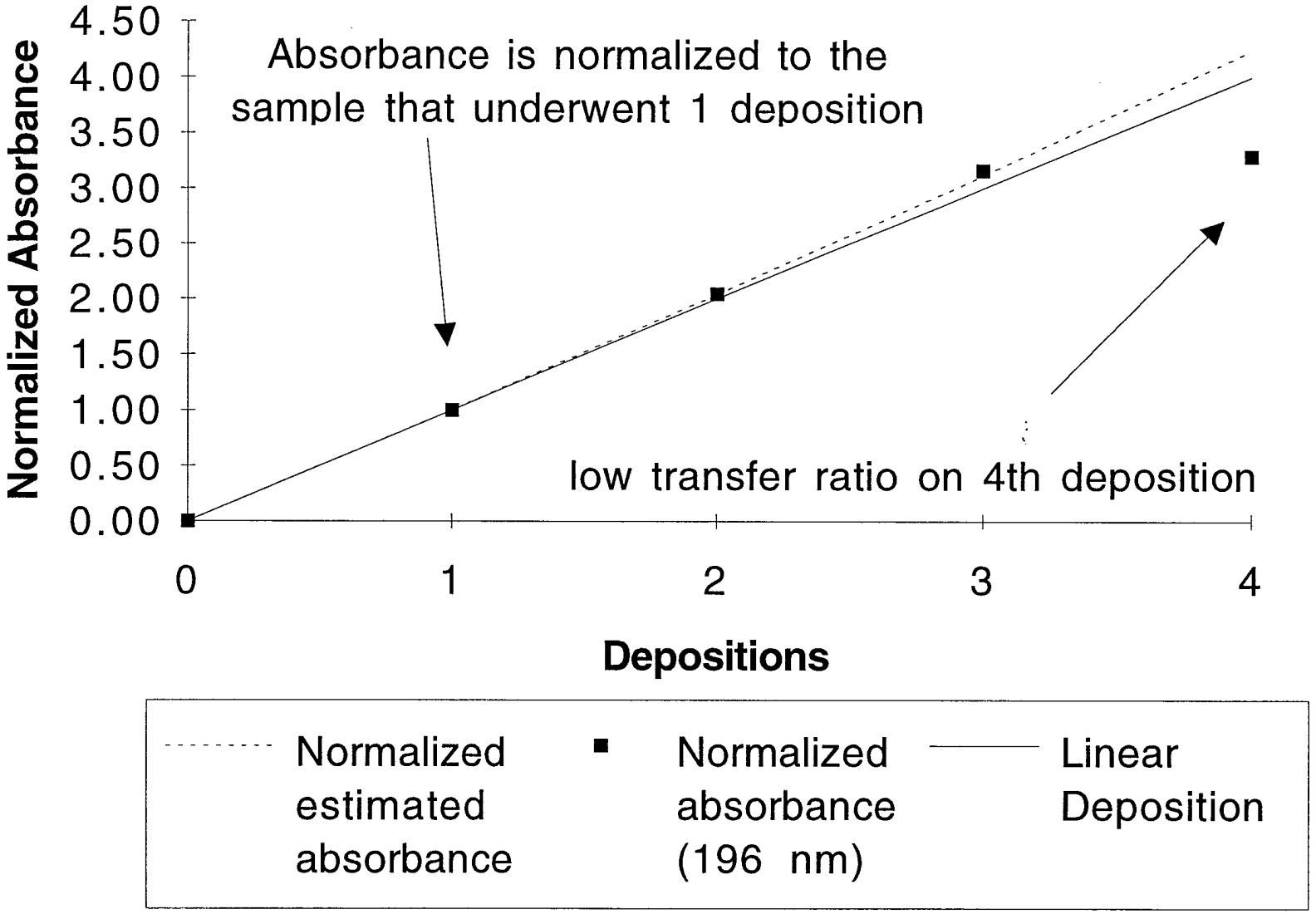

Figure 17 Comparison plot of UV-visible absorbance at 196 nm for the normalized measured and normalized estimated absorbances

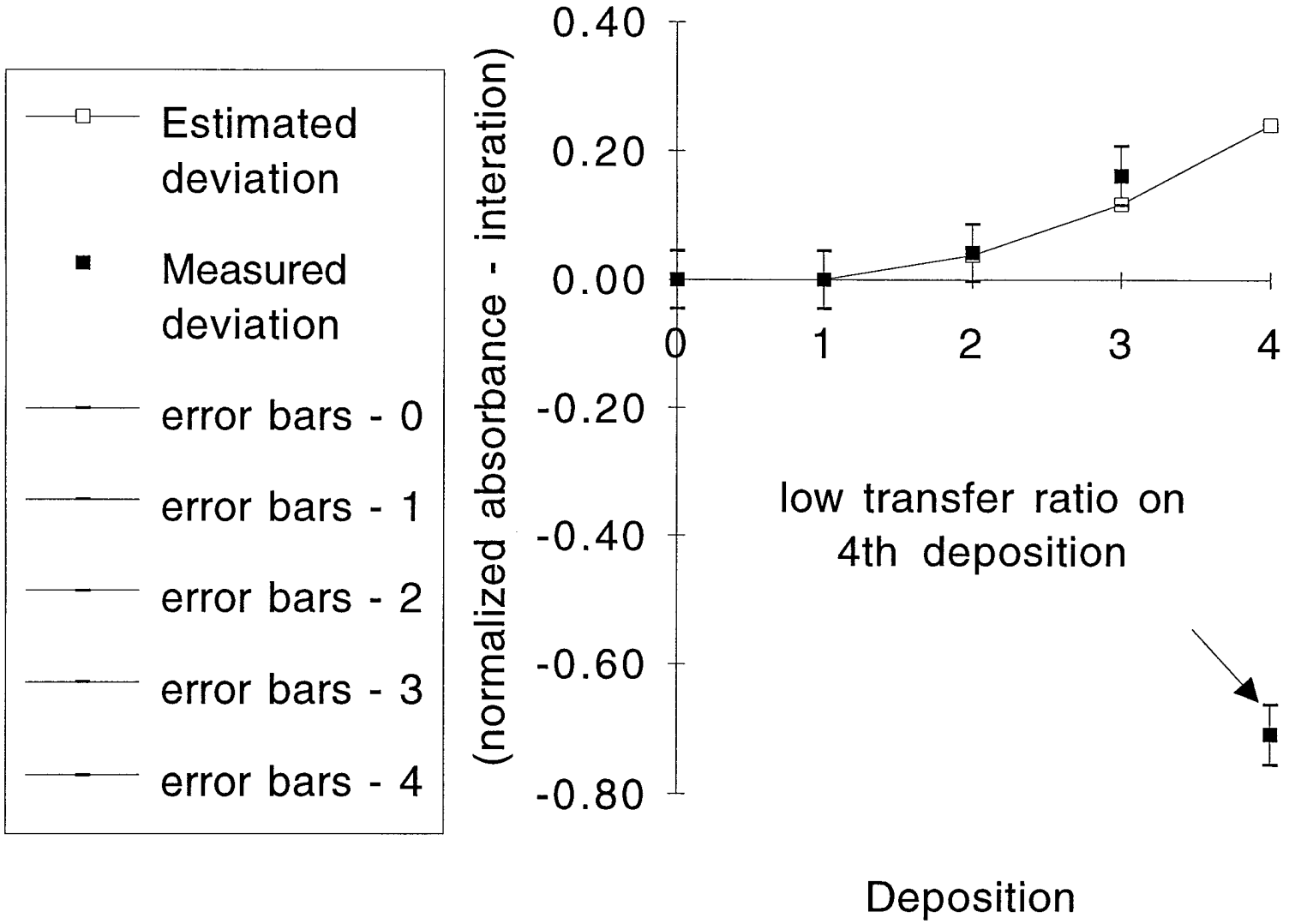

Figure 18 Plot of (normalized absorbance - deposition interation) vs. number of depositions

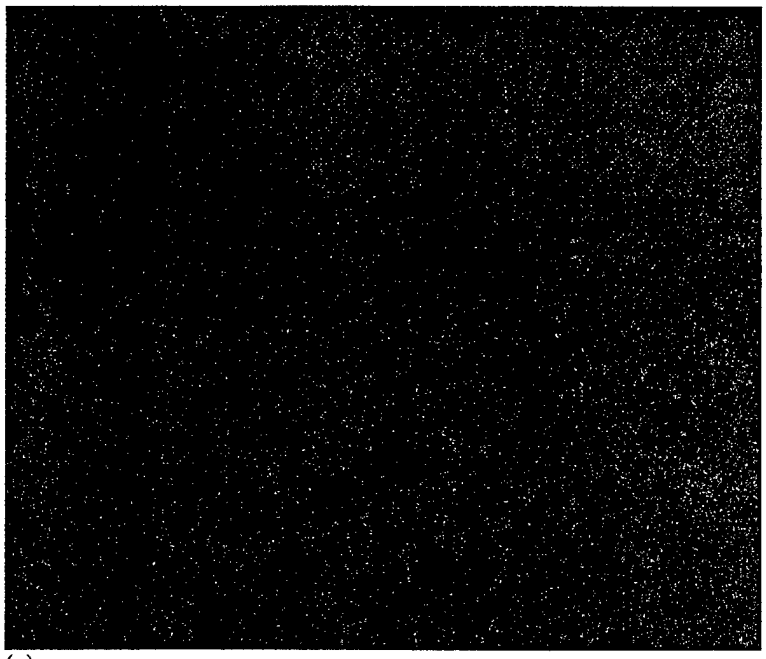

(a)

(b)

19
Figure ~~3.20~~ BAM images of the PPV - precursor film (a) at 10.4 mN/m, and (b) at 25 mN/m with "dust" particles (image enhanced algorithm)

(A high resolution copy will be provided later in the editing process.)

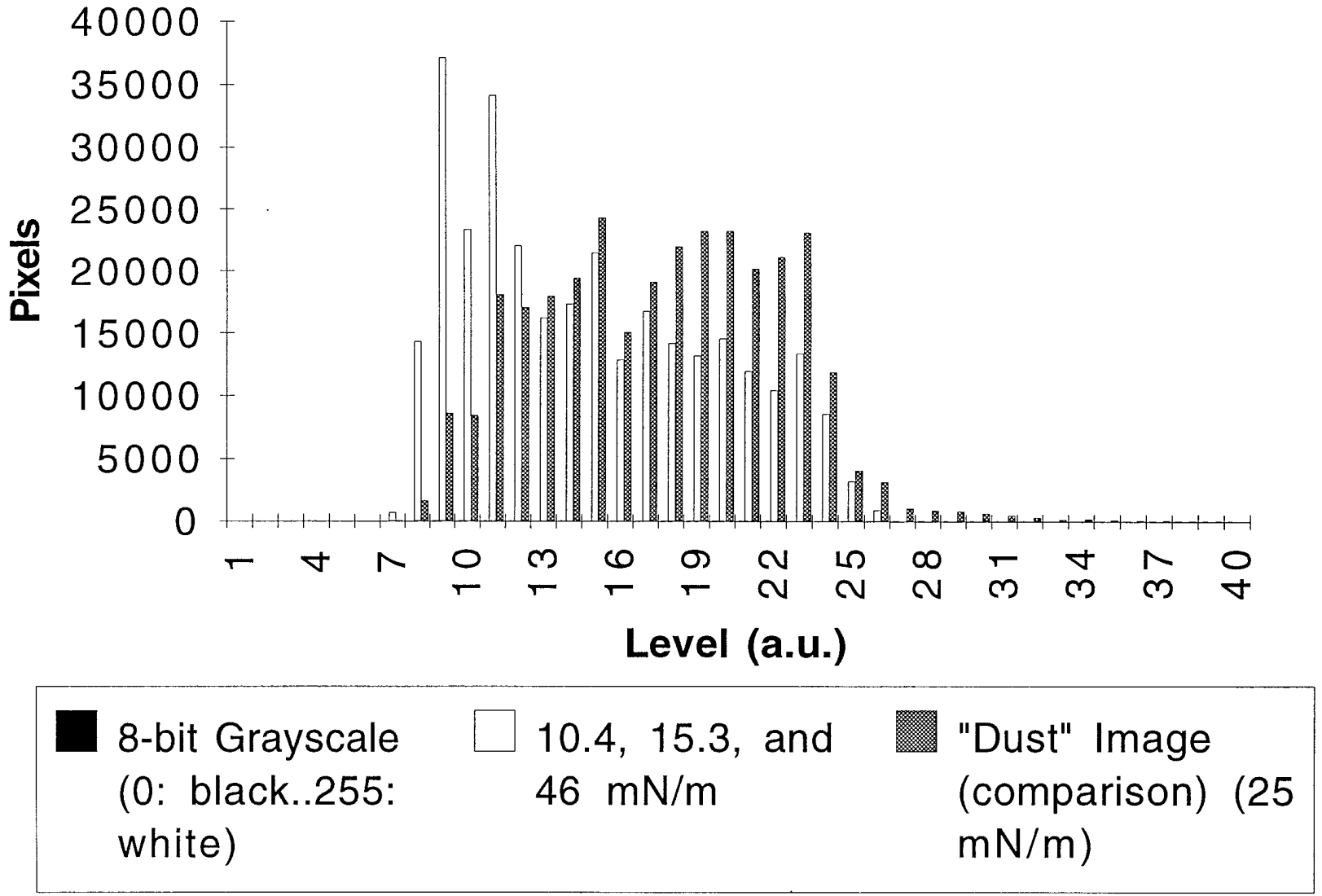

Figure 20 Histogram of pixel intensity for BAM images of the PPV - film at various pressures

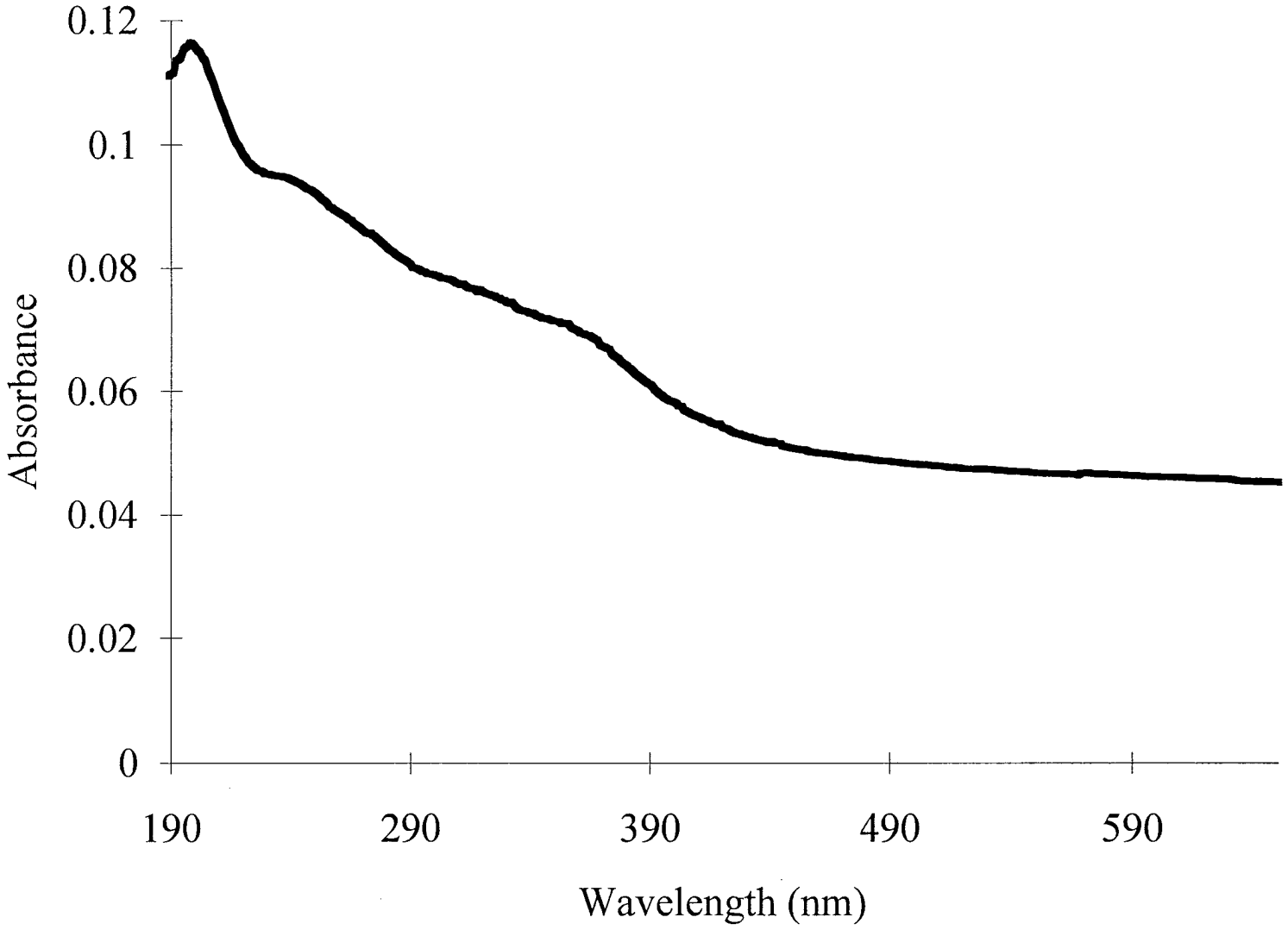

Figure 21 UV - visible absorbance spectrum of a 5 deposition sample doped with ferric chloride

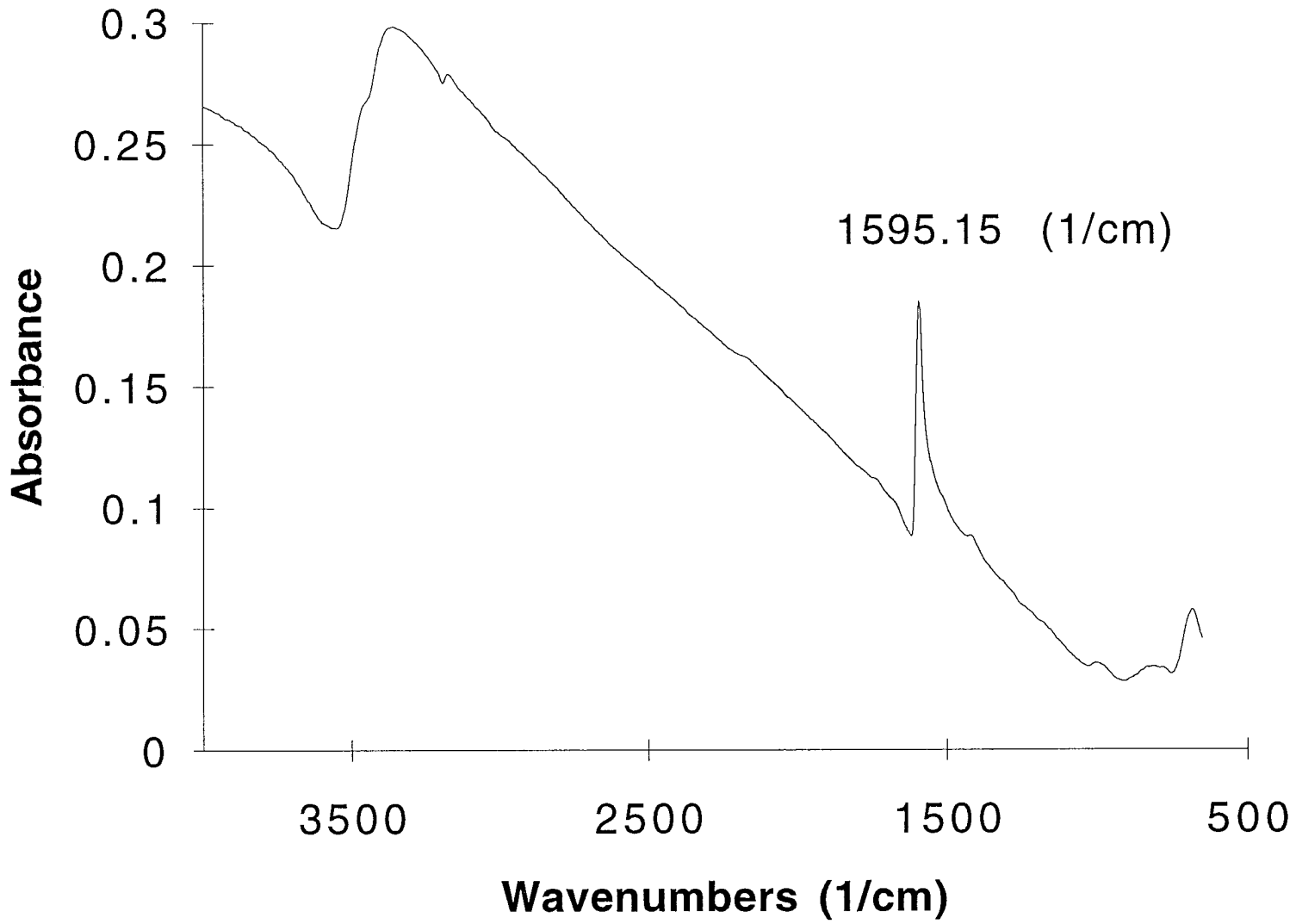

Figure 22 IR-absorbance spectra for a PPV sample doped with ferric chloride